Volume 62
Number 34
5 May 2026
Pages 8521–8778

ChemComm

Chemical Communications

rsc.li/chemcomm

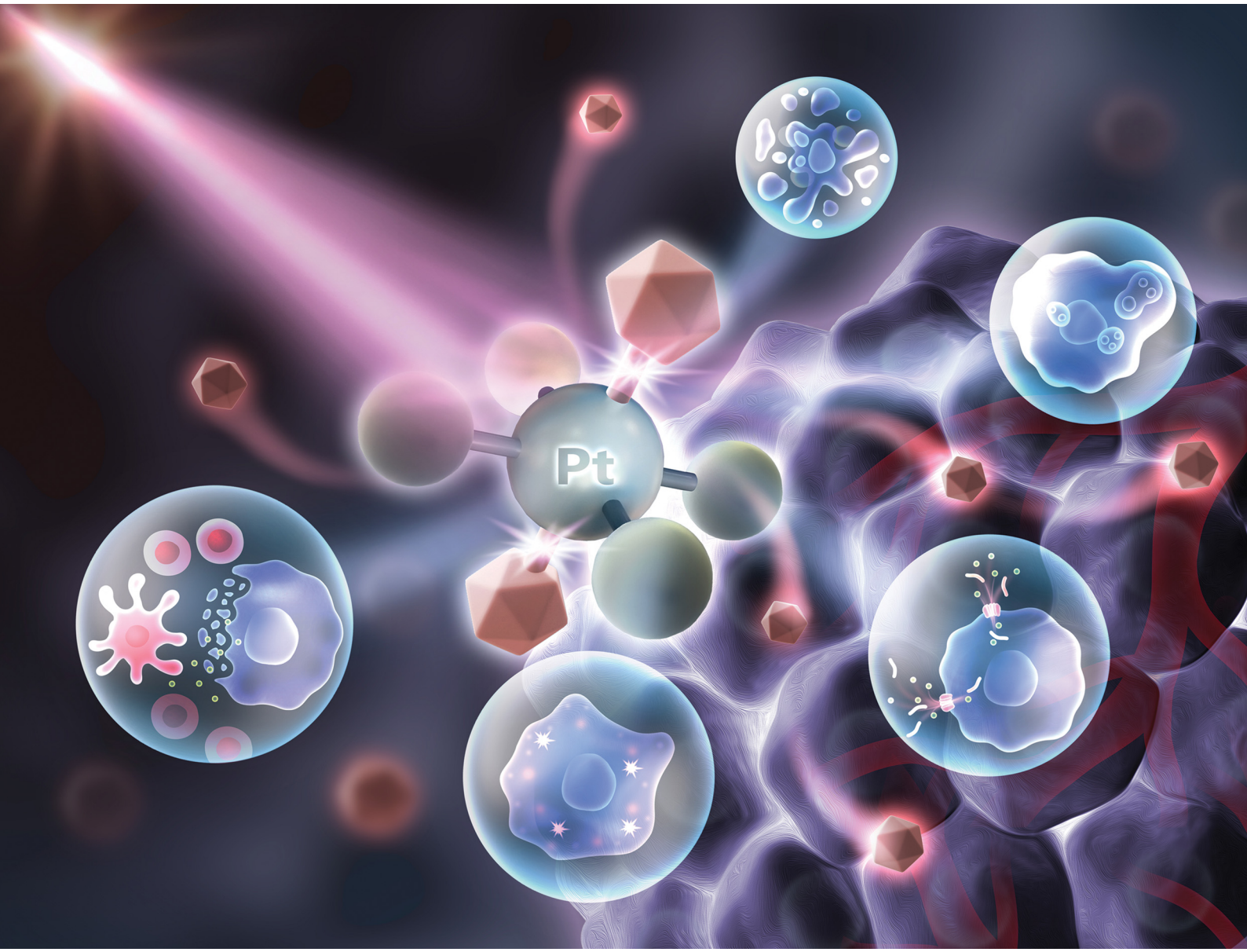

ISSN 1359-7345

ROYAL SOCIETY OF CHEMISTRY

FEATURE ARTICLE

Zhigang Wang, Guangyu Zhu *et al.*

Beyond apoptosis: platinum phototherapeutics overcome resistance by triggering diverse cell death pathways

ChemComm

FEATURE ARTICLE

View Article Online
View Journal | View Issue

Cite this: *Chem. Commun.*, 2026, **62**, 8533

Beyond apoptosis: platinum phototherapeutics overcome resistance by triggering diverse cell death pathways

Shu Chen,[ab] Zhigang Wang *[c] and Guangyu Zhu *[ab]

Platinum (Pt)-based drugs remain the cornerstone of malignant tumor treatment, but are severely constrained by drug resistance. Conventional Pt agents primarily induce apoptosis, yet resistant cancer cells can bypass this pathway, leading to treatment failure. In contrast, phototherapeutic Pt complexes, leveraging photodynamic therapy and photoactivated chemotherapy, represent a novel approach to overcoming resistance by either enhancing apoptosis or activating alternative programmed cell death (PCD) pathways. This review provides a comprehensive overview of Pt-based photosensitizers and photoactivated agents that trigger diverse PCD pathways, including apoptosis, autophagy, ferroptosis, pyroptosis, and immunogenic cell death, to combat resistance. We elucidate the unique features and mechanistic underpinnings of each pathway, providing in-depth analyses of representative complexes to illustrate their PCD induction strategies and effectiveness in reducing resistance. Finally, we present critical insights into and forward-looking perspectives on the development of next-generation Pt phototherapeutics that leverage diverse PCD pathways. Overall, this review highlights the significance of multimodal PCD induction, proposing that targeting these pathways offers a novel strategic opportunity for Pt-based anticancer agents to overcome drug resistance.

Received 15th January 2026,
Accepted 16th March 2026

DOI: 10.1039/d6cc00284f

rsc.li/chemcomm

[a] *Department of Chemistry, City University of Hong Kong, 83 Tat Chee Avenue, Hong Kong SAR 999077, People's Republic of China. E-mail: guangzhu@cityu.edu.hk*
[b] *City University of Hong Kong Shenzhen Research Institute, Shenzhen 518057, People's Republic of China*
[c] *Nation-Regional Engineering Lab for Synthetic Biology of Medicine, International Cancer Center, School of Pharmacy, Shenzhen University Medical School, Shenzhen 518060, People's Republic of China. E-mail: wangzg@szu.edu.cn*

1. Introduction

Platinum (Pt)-based chemotherapeutic agents, including cisplatin, carboplatin, and oxaliplatin (Fig. 1a), play a pivotal role in modern oncology. They are integral to nearly 50% of chemotherapy regimens and significantly enhance survival rates

Shu Chen

Shu Chen received her BSc in Chemistry (2018) from Nanjing Normal University and completed her PhD at City University of Hong Kong (2023) under the supervision of Prof. Guangyu Zhu. Her doctoral research focused on designing and synthesizing novel platinum(IV) anticancer prodrugs with various linkers and elucidating their activation mechanisms in live cells. She is currently a postdoctoral researcher in Prof. Zhu's research group.

Zhigang Wang

Zhigang Wang received his BSc from China Agricultural University and his MPhil in Chemistry from Nankai University. He obtained his PhD in Chemistry from City University of Hong Kong under the supervision of Prof. Guangyu Zhu. After completing his doctoral studies, he joined the School of Pharmaceutical Sciences at Shenzhen University as an Assistant Professor and was promoted to an Associate Professor in 2024. His research focuses on metal-based complexes for cancer immunotherapy and stimuli-responsive photochemotherapeutics for photoactivated chemotherapy.

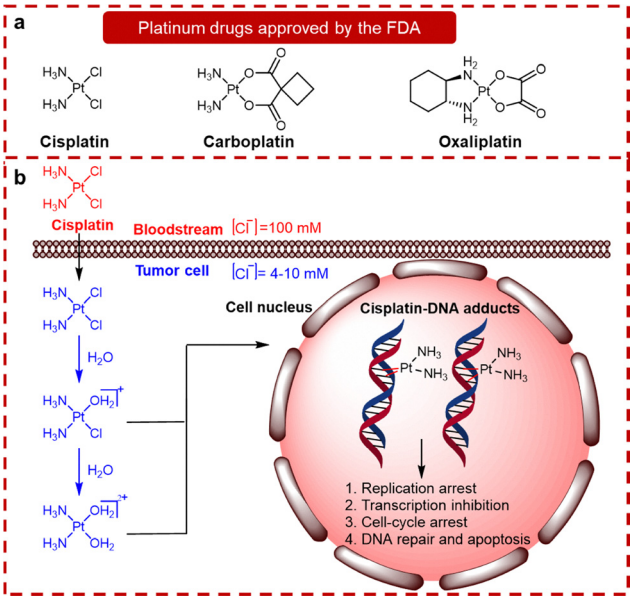

Fig. 1 (a) The chemical structures of the FDA-approved Pt(II) drugs. (b) The mechanism of cisplatin and related Pt-based anticancer drugs involves a four-step process: cellular uptake, activation/aquation, DNA binding, and the cellular processing of the resulting DNA damage that ultimately triggers apoptosis.[14]

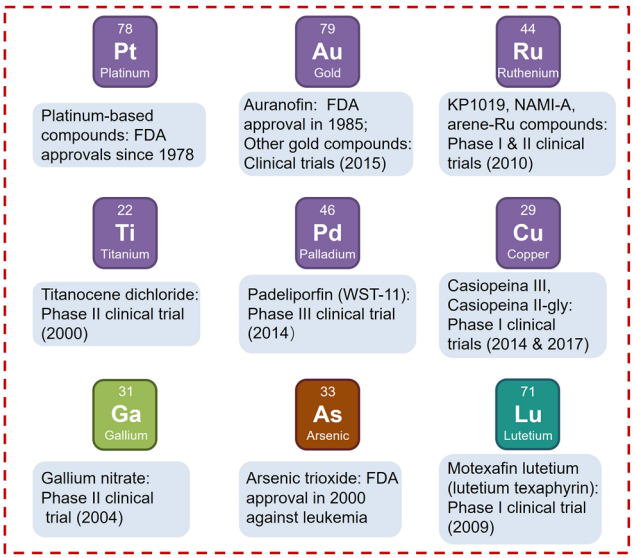

Fig. 2 The metal-based drugs that have entered clinical trials.[23,27]

across various cancer types.[1–3] Driven by this established therapeutic success, extensive research has focused on understanding their molecular mechanisms and developing innovative Pt-based complexes to further augment anticancer efficacy.[4–6] It is widely acknowledged that Pt-based anticancer drugs enter cells primarily through passive diffusion or active transport *via* specific transporters, notably copper transporter 1 (Ctr1) for cisplatin and organic cation transporters (OCTs) for oxaliplatin.[7–9] Once inside the cell, these drugs undergo aquation (Fig. 1b), forming intrastrand and interstrand cross-links with purine bases in nuclear DNA.[9,10] These Pt–DNA adducts distort the DNA double helix, hindering vital processes such as replication and transcription. This disruption triggers cellular stress responses, often culminating in apoptosis.[11–13]

Pt complexes hold a central position among metal-based anticancer agents, underscored by three key advantages that remain unmatched by other metals at a similar scale.[15] First, Pt drugs have an unparalleled record of regulatory approval and clinical use.[16] Since the discovery of cisplatin's antitumor activity in the late 1960s, three generations of Pt drugs have received FDA approval and become first-line therapies for multiple solid tumors.[1] Second, Pt's therapeutic efficacy stems from distinctive ligand-exchange kinetics paired with a well-defined mechanism of action. Pt(II) complexes display moderate ligand-exchange rates that balance stability in the extracellular, chloride-rich environment with sufficient reactivity for intracellular activation and formation of durable DNA adducts, which finally induce cell-cycle arrest and apoptosis.[12,17] Comparable kinetics are rarely achieved by other metals, as decades of structure–activity relationship studies have delivered limited clinical success for non-Pt alternatives.[18–20] Third, except arsenic trioxide, no non-Pt metal-based drug has yet gained FDA approval specifically for cancer therapy (Fig. 2). Most remain in preclinical or early-phase clinical development because of shortcomings compared to Pt drugs. For instance, Pd(II) analogs—despite structural similarity to Pt(II)—undergo ligand substitution 10^4–10^5 times faster, rendering them prone to thiol-mediated deactivation before reaching nuclear DNA and consequently resulting in poor antitumor efficacy.[21,22] Likewise, Au(III) complexes explored as cisplatin alternatives have proven relatively unstable, readily reducing to metallic gold under physiological conditions.[23–25] Although ruthenium compounds are the most promising non-Pt candidates, with lower toxicity and selective anticancer activity, they still lack large phase III trials and the decades of clinical validation that underpin Pt drugs.[26] Overall, while non-Pt metals may offer

Guangyu Zhu

Guangyu Zhu obtained his BSc in Chemistry from Peking University (2002), where he developed a strong passion for biological chemistry and drug discovery. He obtained a PhD in Biological Chemistry from the Department of Chemistry at the University of Pittsburgh (2007), followed by postdoctoral training at the Massachusetts Institute of Technology (MIT). He joined City University of Hong Kong in 2011 and is currently Head of Department and Professor. His research interest lies at the interface of chemistry and biology, focusing on anticancer drug development and mechanisms.

benefits such as reduced toxicity and novel mechanisms, none has matched the proven efficacy, clinical versatility, and global therapeutic impact of Pt complexes in oncology so far.

Despite its success, the efficacy of Pt-based chemotherapy is often severely compromised by intrinsic or acquired drug resistance, which contributes to treatment failure in over 90% of cases.[28–31] Resistance mechanisms are diverse and include reduced drug uptake, enhanced efflux, increased intracellular detoxification, augmented DNA damage repair capacity, and the downregulation or blockade of apoptosis.[1,32–35] Among these, defective apoptosis is particularly consequential, as it operates downstream of Pt–DNA adduct formation and directly counteracts cytotoxicity.[32] In resistant cancers, apoptotic dysfunction commonly involves the overexpression of anti-apoptotic proteins (*e.g.*, Bcl-2 and Bcl-xL), loss or inactivation of pro-apoptotic proteins (*e.g.*, BAX), alterations in the p53 pathway, and activation of pro-survival signaling (*e.g.*, PI3K/Akt).[36–38] Accordingly, restoring apoptotic signaling by targeting these mechanisms represents a critical strategy for overcoming Pt resistance.

Beyond restoring apoptosis, engaging alternative cell-death programs offers a complementary route to overcome drug resistance. According to the Nomenclature Committee on Cell Death (NCCD), cell death is broadly classified into accidental cell death (ACD) and regulated cell death (RCD).[39–41] ACD is an uncontrolled biological process triggered by overwhelming physical or chemical insults, whereas RCD, also known as programmed cell death (PCD), involves a highly orchestrated, genetically encoded cascade of molecular events.[42] PCD encompasses apoptosis, autophagy, pyroptosis, ferroptosis, and immunogenic cell death (ICD), among others, and plays critical roles in cancer progression and therapeutic response.[42] These non-apoptotic pathways provide novel therapeutic targets and offer significant opportunities to enhance cancer treatments and mitigate drug resistance.[43]

Overcoming Pt resistance requires complexes that either amplify suppressed apoptotic signaling or activate alternative PCD pathways that remain effective in resistant cells. Photoactivatable Pt complexes offer a means to achieve both goals while addressing key drawbacks of traditional Pt(II) chemotherapeutics, including systemic toxicity, severe side effects, and intrinsic or acquired resistance. The core concept is light-controlled drug action *via* photoactivatable platforms that offer high spatiotemporal precision, on-demand activation, and minimal invasiveness. These complexes are primarily developed based on two strategies: photoactivated chemotherapy (PACT) and photodynamic therapy (PDT). In PACT, inert Pt complexes remain non-toxic in the dark but are selectively activated within light-irradiated tumor tissues to release cytotoxic Pt(II) species, often accompanied by the generation of reactive oxygen species (ROS). The localized, on-demand activation confines therapeutic effects to the tumor site, thereby drastically reducing off-target toxicity relative to traditional Pt regimens.[44–46] In PDT, Pt complexes act as photosensitizers (PSs) that, upon light irradiation, form a triplet excited state which generates cytotoxic ROS *via* two primary pathways: type I photoreaction, involving electron transfer to produce radical species such as superoxide ($O_2^{\bullet-}$) and hydroxyl ($^{\bullet}OH$) radicals, and type II photoreaction, involving energy transfer to molecular oxygen to generate singlet oxygen ($^1O_2$).[47–51] This ability to generate high levels of ROS independent of DNA binding provides a powerful, orthogonal mechanism to overcome classical Pt resistance.

PACT and PDT leverage precise spatiotemporal control to synergize Pt-based cytotoxicity with photoactivated species, amplifying apoptotic signaling. More importantly, they can directly trigger non-apoptotic PCD pathways, which bypass established resistance mechanisms. Specifically, intrinsic apoptotic signaling can be enhanced by generating a lethal flux of ROS that overwhelms mitochondrial defenses. Furthermore, photochemical disruption of lysosomal membranes can initiate autophagic cell death, a non-apoptotic pathway that effectively circumvents common resistance mechanisms. Beyond autophagy, the localized and intense ROS burst generated during the photodynamic process can cause catastrophic oxidative damage to lipids, thereby triggering ferroptosis—an iron-dependent cell death pathway that is impervious to classic apoptotic resistance factors. In parallel, photoactivation can promote ROS generation and activate caspase-1, leading to gasdermin D (GSDMD)-mediated pyroptosis. This highly inflammatory and lytic cell death mode results in plasma membrane rupture and the release of inflammatory contents, thereby effectively compensating for apoptotic defects. Moreover, the cytotoxic species generated during PDT or PACT can induce ICD, characterized by calreticulin (CRT) exposure and the release of damage-associated molecular patterns (DAMPs) such as adenosine triphosphate (ATP) and high-mobility group box 1 (HMGB1). These DAMPs stimulate a robust antitumor immune response, promoting the clearance of cells that would otherwise be resistant.

This review systematically explores the burgeoning field of Pt-based photoactivated agents and PSs engineered to initiate diverse PCD pathways—including apoptosis, autophagy, ferroptosis, pyroptosis, and ICD—as a targeted strategy to surmount drug resistance (Fig. 3). Following a detailed examination of the

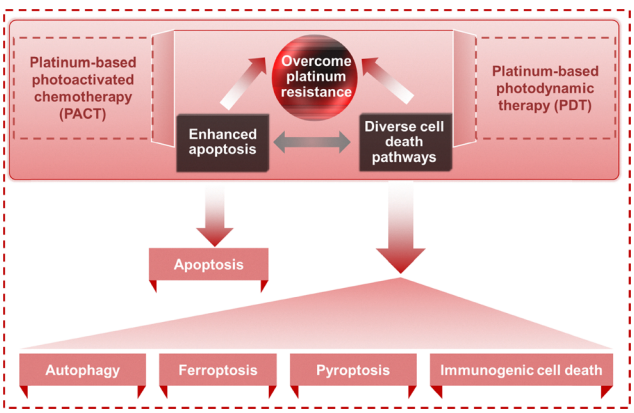

Fig. 3 Illustration of Pt phototherapeutics overcoming resistance by either intensifying apoptotic signals or triggering diverse cell death pathways.

distinct characteristics and mechanisms governing each PCD pathway, we provide in-depth analyses of representative photoactivated Pt complexes to illustrate their specific mechanisms of PCD induction and their potential to circumvent resistance. Finally, we offer a critical summary and a forward-looking perspective on the trajectory for developing next-generation Pt phototherapeutics that leverage novel PCD paradigms to overcome drug resistance. To maintain a focused discussion, Pt-based nanoparticle systems loaded with Pt agents are deliberately excluded, with the focus on small-molecule complexes. This review highlights the induction of diverse cell death modalities as a key therapeutic strategy for circumventing resistance.

2. Pt phototherapeutics that induce apoptosis

Apoptosis, the first described form of PCD, is characterized by distinct morphological changes, including cell shrinkage, membrane blebbing, chromatin condensation, and fragmentation into apoptotic bodies.[52,53] It is classified into caspase-dependent and caspase-independent pathways (Fig. 4).[54] Caspase-dependent apoptosis proceeds through two main pathways: the extrinsic pathway, activated by extracellular stimuli, and the intrinsic pathway, triggered by intracellular stress.[55] The extrinsic pathway is initiated when tumor necrosis factor superfamily (TNFSF) ligands bind to death receptors, forming the death-inducing signaling complex (DISC).[56–58] Within the DISC, procaspase-8 undergoes autoproteolytic cleavage, activating caspase-8, which then activates downstream executioner caspases, primarily caspase-3/7, culminating in extrinsic apoptosis.[59] The intrinsic apoptotic pathway, activated by stressors such as DNA damage and oxidative stress, triggers the activation of pro-apoptotic BCL-2 family proteins (BAX and BAK), which subsequently mediate mitochondrial outer membrane permeabilization (MOMP). This process releases apoptogenic factors such as cytochrome c and apoptosis-inducing factor (AIF). Cytochrome c binds apoptotic protease-activating factor-1 (APAF-1), inducing its oligomerization and recruiting procaspase-9 to form the apoptosome.[60,61] Within the apoptosome, procaspase-9 undergoes autocatalytic activation, which, in turn, activates executioner, primarily caspases-3/7, to complete the intrinsic apoptotic pathway.[59] Concurrently, AIF translocates to the nucleus, causing DNA condensation and fragmentation, indicative of caspase-independent apoptosis.[62] Pt-based anticancer drugs primarily activate the intrinsic pathway by inducing DNA crosslinks and mitochondrial dysfunction, leading to PCD. Furthermore, photoactivatable Pt complexes offer a promising strategy to overcome resistance by generating ROS capable of engaging both intrinsic and extrinsic apoptotic mechanisms.

Pt-based PSs show promise for PDT, but their application is hindered by challenges such as drug resistance and the hypoxic tumor microenvironment.[63,64] To address these limitations, Wang *et al.* developed a naphthalimide-modified cyclometalated Pt(II) complex, PtPAN (complex **1**, Fig. 5).[65] In cisplatin-resistant A549cisR lung cancer cells, complex **1** exhibited only moderate dark toxicity under both normoxia (half-maximum inhibitory concentration IC_{50}: 9.43 ± 0.43 μM) and hypoxia (IC_{50}: 7.92 ± 2.23 μM). Upon near-infrared (NIR) two-photon irradiation, however, photocytotoxicity increased significantly, with IC_{50} values of 1.25 ± 0.39 μM (normoxia) and 0.18 ± 0.08 μM (hypoxia). Notably, the phototherapeutic index (PI, defined as IC_{50} in the dark/IC_{50} under irradiation) reached 44 under hypoxia—approximately six times higher than that under normoxia (PI = 7.54)—demonstrating its efficacy in overcoming limited oxygen availability. Furthermore, complex **1** effectively reduced Pt resistance, as evidenced by low resistance factors (RFs, defined as IC_{50} in resistant cells/IC_{50} in sensitive cells) under irradiation: 0.03 in hypoxia (IC_{50}: 5.92 ± 0.57 μM in A549 and 0.18 ± 0.08 μM in A549cisR) and 0.54 in normoxia (IC_{50}: 2.18 ± 1.21 μM in A549 and 1.25 ± 0.39 μM in A549cisR). Mechanistically, complex **1** exhibits negligible covalent interactions with calf thymus DNA (CT-DNA) in the dark, but efficiently unwinds the DNA superhelix *via* photoinduced production of ROS through a combination of both type I and

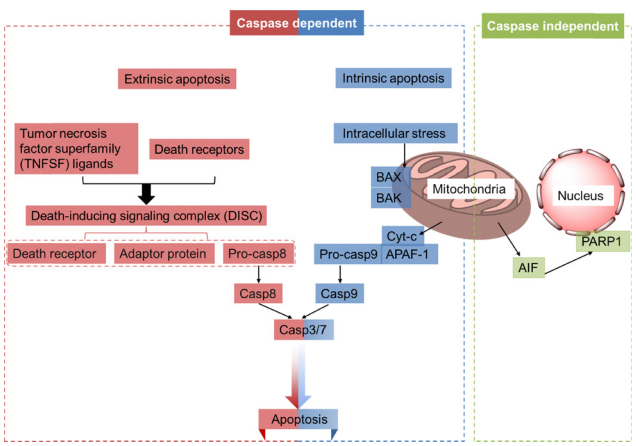

Fig. 4 Apoptotic cell death pathway. Apoptosis can be triggered through several distinct mechanisms: the formation of the death-inducing signaling complex (DISC), mitochondrial damage, or the activation of PARP.

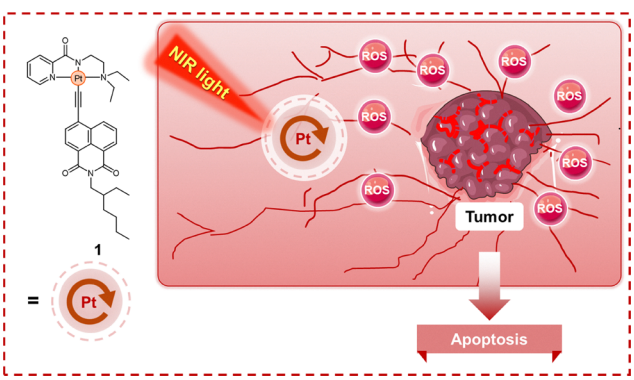

Fig. 5 The structure of complex **1** and its mechanism of action. Its antitumor effect is driven by near-infrared light-induced ROS production, which triggers apoptotic cell death in the tumor cells.

type II photodynamic reactions. This ROS-mediated damage is associated with mitochondrial membrane depolarization and a substantial increase in apoptosis, as evidenced by strong Annexin V-FITC (green) and propidium iodide (red) signals in irradiated cells and negligible signals in dark controls. Flow cytometry confirmed this shift, with the percentage of apoptotic cells rising to 34.0% post-irradiation compared to 4.70% in the dark. *In vivo* studies further underscore the potential of complex **1** as a two-photon-activated PS, demonstrating near-complete tumor eradication with minimal systemic toxicity. These findings position complex **1** as a Pt-based phototherapeutic that surmounts both hypoxic limitations and cisplatin resistance through ROS-driven cell death induced by type I and type II photodynamic pathways, thereby bypassing the primary resistance pathways associated with conventional Pt chemotherapeutics.

The clinical success of Pt(II)-based chemotherapeutics has spurred the development of Pt(IV) prodrugs, which are designed to reduce adverse effects and improve pharmacological performance by undergoing reduction specifically within cancer cells.[66–69] Concurrently, Ru(II) polypyridyl complexes have emerged as promising PSs for PDT due to their superior tunability and photochemical properties.[70–72] Heterobimetallic complexes incorporating Pt with a second metal represent a significant advancement in anticancer metallodrug design, as they integrate Pt's core cytotoxic mechanism with complementary actions from the secondary metal to broaden the therapeutic profile and overcome platinum resistance.[73] Building on these advances, Gasser, Gibson, and colleagues developed a novel Pt(IV)–Ru(II) conjugate (**2**, Fig. 6) to combine cancer-activated chemotherapy with PDT.[74] Complex **2** entered cells primarily *via* energy-dependent endocytosis. Following internalization and reduction of the Pt(IV) center, the constituent metals exhibited distinct subcellular localization: Pt accumulated primarily in the nucleus, while Ru localized predominantly to the Golgi apparatus. Upon irradiation, the Golgi-localized Ru species generated singlet oxygen, thereby exerting PDT effects. This combined action conferred potent photo-induced cytotoxicity in ovarian carcinoma A2780 cells and their resistant variants—A2780cisR (cisplatin-resistant) and A2780ADR (doxorubicin-resistant)—with IC_{50} values of 0.08–0.10 μM (480 nm) and 0.16–0.19 μM (595 nm). Notably, it significantly overcame resistance, showing RFs of 1.25 (480 nm) and 1.19 (595 nm) in A2780cisR/A2780 and 1.12 (480 nm) and 1.06 (595 nm) in A2780ADR/A2780. In contrast, cisplatin yielded substantially higher RF values of 4.30 and 1.98, respectively. Mechanistic studies revealed that apoptosis induced by cisplatin and complex **2** in the dark likely proceeded *via* the ERK/p53/PUMA pathway, as evidenced by the unaffected caspase-3/7 activity. In contrast, irradiated complex **2** significantly increased caspase-3/7 activity, suggesting a shift to a different photoactivated apoptotic mechanism. This shift may account for the potent ability of irradiated complex **2** to overcome resistance. Moreover, the marked rescue of cell viability by both apoptotic and paraptotic inhibitors upon irradiation implicates concurrent activation of these two death pathways. Complex **2** effectively penetrated multicellular tumor spheroids (MCTS), retaining dark cytotoxicity (IC_{50} = 7.32 μM) and achieving nanomolar phototoxicity (IC_{50} = 0.49–0.68 μM). This dual-action conjugate represents a promising strategy for overcoming resistance in cancer therapy and warrants further development.

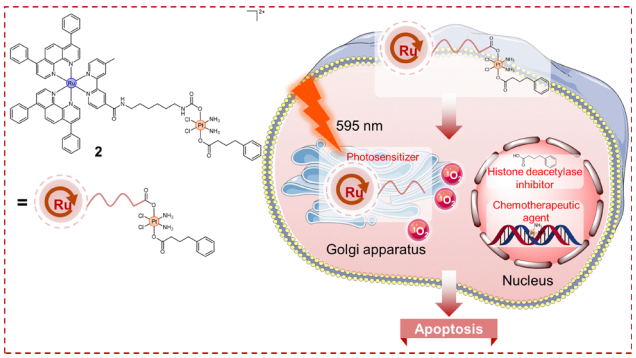

Fig. 6 The chemical structure of Pt(IV)–Ru(II) conjugate **2** and its mechanism of action. Upon cellular entry, the Pt(IV) prodrug is reduced to active cisplatin, releasing axial phenylbutyrate and a Ru(II) photosensitizer. Phenylbutyrate inhibits histone deacetylase (HDAC) and chromatin decondensation, enhancing cisplatin–DNA binding. The Ru(II) complex localizes in the Golgi apparatus and, upon irradiation at 595 nm, catalytically generates singlet oxygen. This multi-targeting strategy, inducing cell death *via* concurrent apoptosis and paraptosis, results in potent photocytotoxicity in 2D monolayers and 3D spheroids, demonstrating synergistic action and the ability to overcome drug resistance.

The prevailing approach for enhancing the anticancer activity of Pt(IV) complexes focuses on axial functionalization; however, the photocytotoxic efficacy of diazido Pt(IV) systems is profoundly affected by the choice of equatorial ligands, which govern their photoactivation dynamics.[75–77] Nitroimidazole antibiotics, traditionally used to treat anaerobic infections, have recently gained recognition for their anticancer potential.[78–80] In this context, Sadler, Shi, and Clarkson developed a diazido Pt(IV) prodrug (complex **3**, Fig. 7) featuring two equatorial 1-methyl-5-nitroimidazole ligands.[81] Complex **3** demonstrated potent and oxygen-independent photocytotoxicity under blue-light irradiation (IC_{50} < 5 μM) against bladder cancer cells, while exhibiting low dark toxicity and high selectivity over normal bladder cells (with IC_{50} values 3–20 times higher). Critically, it displayed a pronounced ability to circumvent cisplatin resistance, maintaining efficacy across varying oxygen concentrations. Its cytotoxicity upon blue light irradiation (465 nm) remained consistent across A2780 (IC_{50}: 2.9 ± 0.9 μM under normoxia and 1.7 ± 0.6 μM under hypoxia) and cisplatin-resistant A2780cisR cells (IC_{50}: 0.84 ± 0.06 μM under normoxia and 1.7 ± 0.3 μM under hypoxia), resulting in RFs of 0.29 and 1.0 in normoxia and hypoxia, respectively. By contrast, cisplatin showed an approximately 10-fold decrease in potency against A2780cisR cells, underscoring complex **3**'s superior resistance-bypassing profile. Mechanistically, photoactivated complex **3** generated significant ROS and subsequently induced apoptosis in SW780 bladder cancer cells under normoxic conditions, with early apoptosis increasing from 1.49% to 8.11%

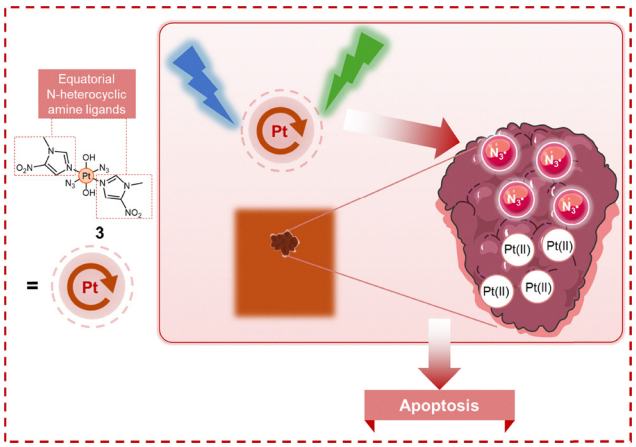

Fig. 7 The chemical structure of complex **3** and its mechanism of action. Complex **3** demonstrates high dark stability and undergoes photoactivation upon irradiation of green or blue light, yielding azidyl radicals. This distinct mechanism triggers photoinduced apoptosis and overcomes cisplatin resistance.

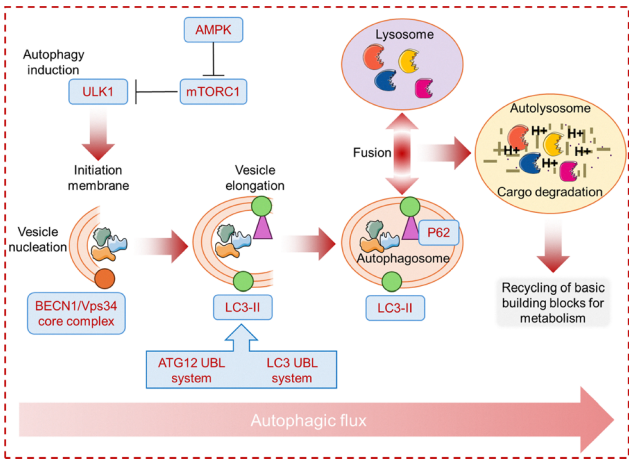

Fig. 8 Schematic of the autophagic pathway. The process is characterized by four key stages: initiation and nucleation of the phagophore, its elongation to engulf cytoplasmic cargo, closure to form a double-membraned autophagosome, and finally, fusion with a lysosome to form an autolysosome for component degradation and recycling.

and late apoptosis from 6.67% to 45.82% relative to dark controls. This pronounced apoptotic response may account for the observed reversal of drug resistance under normoxia. In contrast, under hypoxia, complex **3** did not primarily induce apoptosis but instead promoted nuclear Pt accumulation and exacerbated mitochondrial membrane depolarization. These alternative mechanisms collectively contribute to overcoming both cisplatin- and hypoxia-mediated resistance. In addition to its cellular effects, complex **3** exhibited high liver microsomal stability and photo-enhanced Pt accumulation in rat bladder tissue, underscoring its potential for clinical translation as a phototherapeutic agent for bladder cancer. These findings establish equatorial nitroimidazole ligands as a viable strategy to enhance the photocytotoxicity of diazido Pt(IV) complexes, thereby overcoming dual resistance mechanisms and advancing the development of phototherapeutic Pt drug candidates.

3. Pt phototherapeutics that induce autophagy

Autophagy is a conserved catabolic process vital for cellular homeostasis, acting as a double-edged sword: it promotes cell survival under stress but induces cell death when dysregulated.[82,83] Autophagy is triggered by stimuli such as nutrient or growth factor deprivation, infection, and organelle damage, and it regulates cell development, differentiation, and tissue remodelling.[84] Among its various forms, macroautophagy (hereafter referred to as autophagy) is the most prevalent and involves the formation of double-membraned autophagosomes that engulf cytoplasmic cargo for lysosomal degradation.[54] The process proceeds through initiation, nucleation, elongation, autophagosome closure, and autolysosome formation (Fig. 8).[85,86] Initiation is mediated by the ULK1 complex, followed by nucleation, which requires the BECN1/Vps34 lipid-kinase complex. Phagophore elongation employs ATG12 and light chain 3 (LC3) conjugation systems, in which LC3-I is lipidated to LC3-II—a canonical autophagosomal marker. The adaptor p62 binds ubiquitinated cargo and LC3-II,[87] delivering substrates for degradation; accordingly, p62 accumulation signifies impaired autophagic flux.[88] After lysosomal fusion, degraded materials are recycled to sustain metabolism and stress adaptation.[89] Conversely, dysregulated flux disrupts proteostasis and homeostasis, promoting cell death.[90] This functional duality underpins the therapeutic relevance of autophagy in cancer. Specifically, the induction of autophagy represents a promising avenue for countering Pt resistance in oncology. This mechanism can overcome resistance either by activating alternative, non-apoptotic cell death pathways or by selectively degrading pro-survival proteins that contribute to chemoresistance. Therefore, the rational design of novel Pt complexes that potently induce autophagy offers a strategic approach to re-sensitizing tumors to conventional chemotherapy and thereby improving chemotherapeutic efficacy against resistant cancers.

The therapeutic potential of heterobimetallic complexes in PDT stems from their tunable photophysical properties.[73,91] By leveraging synergistic intermetallic interactions, achieved through deliberate metal selection and ligand design, these complexes offer a superior alternative to conventional monometallic metallodrugs.[92–94] A notable example is the work by Kumbhar *et al.*, who developed heterobimetallic Ru(II)–Pt(II) polypyridyl complexes $[Ru(bpy)_2(BPIMBp)PtCl_2]_2$ (**4**, Fig. 9) and $[Ru(phen)_2(BPIMBp)PtCl_2]_2$ (**5**, Fig. 9).[95] Cell-based studies revealed potent photocytotoxicity in MCF-7 cells ($IC_{50} < 20$ μM) upon irradiation at 450 nm, while maintaining low dark toxicity ($IC_{50} > 300$ μM). Because Pt-resistant cancers frequently exploit basal autophagy for survival,[96] pharmacological modulation of autophagy – either by inhibiting cytoprotective flux or by inducing lethal autophagy – has emerged as a strategy to overcome chemoresistance.[97] Motivated by this rationale, the

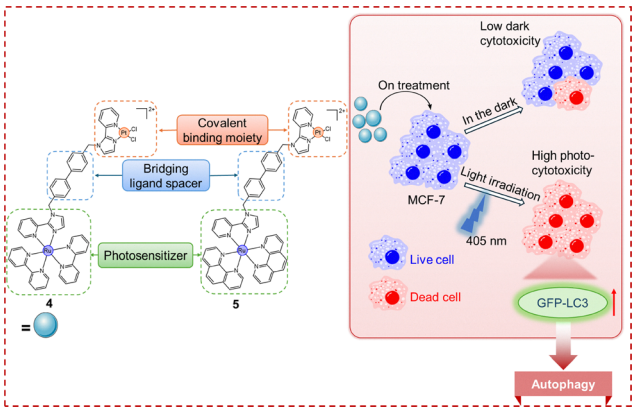

Fig. 9 Design, structure–activity relationship, and mechanism of action of Ru(II)–Pt(II) complexes **4** and **5**. The complexes act as potent photosensitizers, demonstrating light-activated cytotoxicity (λ = 405 nm) in MCF-7 cells through the induction of autophagy, while remaining non-toxic in the dark.

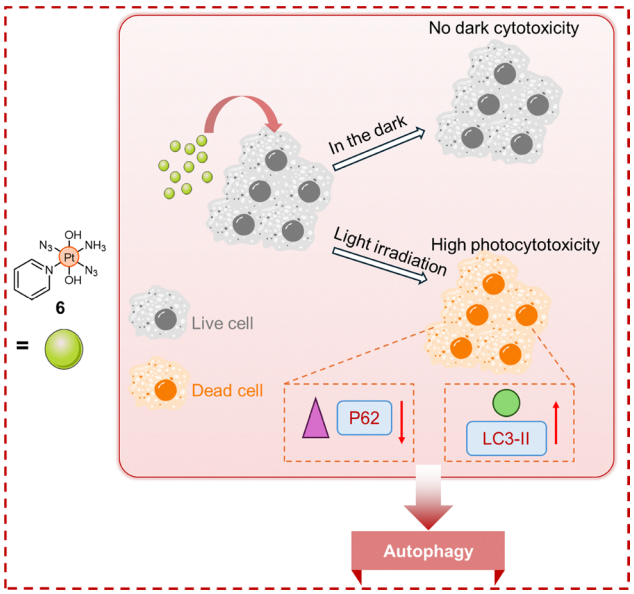

Fig. 10 The chemical structure of complex **6** and its mechanism of action. UVA irradiation activates complex **6**, inducing cytotoxic autophagy in HL-60 cells, as evidenced by increased LC3B-II and decreased p62 protein levels. This photoinduced mechanism is distinct from that of cisplatin, highlighting the potential for novel, light-activated pathways to overcome drug resistance.

authors investigated whether complexes **4** and **5** act as autophagy-modulating chemosensitizers to trigger autophagic cell death and thereby potentially overcome drug resistance. To monitor autophagy induction, the authors quantified microtubule-associated protein 1A/1B-LC3 fluorescence, using GFP-LC3 puncta formation as a marker. Treatment with complex **4** induced approximately a 3-fold increase in GFP-LC3 fluorescence in MCF-7 cells, while complex **5** induced approximately a 2-fold increase, both significantly exceeding the cisplatin-induced autophagy. These results suggest that the Ru-polypyridyl PS component of complexes **4** and **5** may partially overcome cisplatin resistance by inducing autophagy in cancer cells, although further detailed investigation is needed to confirm this.

Pt(IV) diazido complexes, designed for photoactivation, exhibit distinctive photobiological properties.[98] As reported by Bednarski and Sadler *et al.*, *trans*,*trans*,*trans*-[$Pt(N_3)_2(OH)_2$-(py)(NH_3)] (complex **6**, Fig. 10) is a highly effective photoactivated anticancer agent, displaying significant cytotoxicity against a panel of human cancer cells when exposed to UVA irradiation, while remaining non-toxic in the dark.[99] The mechanism underlying the light-induced cytotoxicity for complex **6** is distinct from that of cisplatin. First, complex **6** exhibited no cross-resistance in three cell lines resistant to oxoplatin (*cis*,*trans*,*cis*-[$PtCl_2(OH)_2(NH_3)_2$], a Pt(IV) prodrug derived from cisplatin), with RFs ranging from 0.88 to 1.20. In contrast, cisplatin exhibited complete cross-resistance in the same cell lines, with RFs of 2.07–2.89. Second, morphological changes in HL-60 cells treated with complex **6** differed significantly from those induced by cisplatin or etoposide,[100,101] a topoisomerase II inhibitor used as a positive control for apoptosis. While cisplatin and etoposide induced characteristic apoptotic features, such as cell shrinkage, membrane blebbing, and caspase-3 activation, complex **6**-treated cells exhibited slight swelling without apoptotic markers. Annexin V/propidium iodide assays further confirmed the absence of apoptosis in cells treated with complex **6** following UVA irradiation. Moreover, at IC_{90} concentrations, cisplatin and etoposide induced S–G_2 and G_2–M cell cycle arrests, respectively, whereas complex **6** exerted a minimal impact on cell cycle distribution. Notably, autophagy appeared to play a central role in the cytotoxicity of UVA-activated complex **6**. HL-60 cells exposed to the activated complex for 6 hours showed a marked increase in LC3B-II levels and a corresponding decrease in p62 levels, consistent with autophagic activation. These findings provide novel insights, demonstrating that the photoinduced cytotoxicity of *trans*-diazido Pt(IV) complexes proceeds *via* an autophagy-mediated pathway distinct from cisplatin's mechanism, thereby presenting a promising strategy to circumvent Pt resistance.

4. Pt phototherapeutics that induce ferroptosis

Ferroptosis is an iron-dependent form of regulated cell death driven by lethal accumulation of lipid peroxides (Fig. 11).[102] Its core mechanism is intrinsically tied to cellular iron metabolism: extracellular Fe^{3+} bound to transferrin is imported *via* transferrin receptor 1 (TFR1), reduced to Fe^{2+} by STEAP3 in endosomes, and released into the labile iron pool by divalent metal transporter 1 (DMT1).[103] The availability of this redox-active iron can be further modulated by phosphorylase kinase catalytic subunit gamma 2 (PHKG2).[104] Excess Fe^{2+} promotes lipid peroxidation (LPO) through Fenton and Fenton-like chemistry, while enzymatic peroxidation of polyunsaturated fatty acids (PUFAs) by lipoxygenases (LOXs) also contributes.[105] A primary defense against ferroptosis is mediated by glutathione

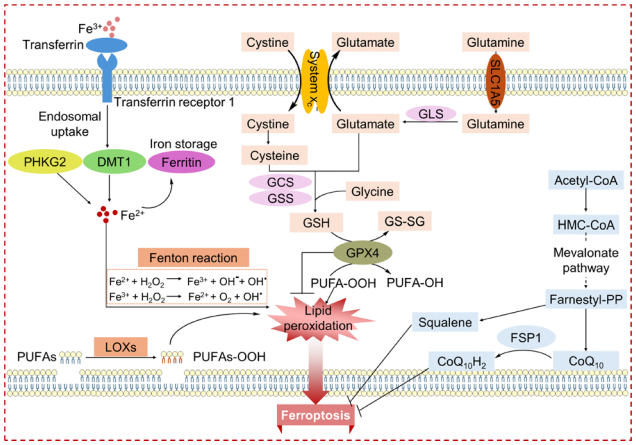

Fig. 11 The ferroptosis cell death pathway. Ferroptosis is characterized by iron-dependent, oxidative cell death triggered by the accumulation of lipid peroxides. Key initiators include inhibition of the cystine/glutamate antiporter (system X_c^-) or the antioxidant enzyme GPX4. The execution phase requires free iron and the peroxidation of polyunsaturated fatty acids (PUFAs). Additionally, the mevalonate pathway contributes to regulation by synthesizing cofactors that suppress ferroptosis.

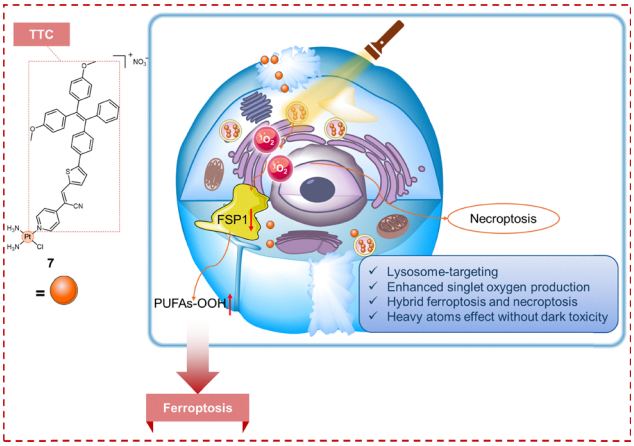

Fig. 12 Chemical structure and mechanism of action of complex **7**, an AIE-active monofunctional Pt(II) photodynamic agent. It enters HeLa cells *via* endocytosis and localizes in lysosomes. Upon light irradiation, it induces downregulation of FSP1 and accumulation of lipid peroxides, triggering synergistic ferroptosis and necroptosis. This mechanism effectively inhibits tumor growth with negligible dark toxicity and overcomes apoptosis resistance.

peroxidase GPX4, which utilizes reduced glutathione (GSH) to reduce lipid hydroperoxides (LOOHs) to non-toxic lipid alcohols.[106,107] GPX4 activity requires adequate GSH, whose synthesis depends on cysteine, primarily imported as cystine *via* the system X_c^- antiporter.[108,109] Inhibition of system X_c^- (*e.g.*, by erastin) or direct GPX4 inactivation (*e.g.*, by RAS-selective lethal 3) causes lethal LOOH accumulation. GSH levels are further modulated by glutamine uptake through SLC1A5 and its conversion to glutamate by glutaminase (GLS).[110] Beyond GPX4, ferroptosis suppressor protein 1 (FSP1) provides an independent protective axis:[110] myristoylated FSP1 regenerates the radical-trapping antioxidant ubiquinol from ubiquinone using NAD(P)H, thereby suppressing LPO propagation.[111] This underscores the protective roles of metabolites such as ubiquinol, squalene, and coenzyme Q10 (CoQ10), which are produced *via* the mevalonate pathway.[112,113] Therapeutically, ferroptosis induction represents a promising strategy to mitigate Pt resistance. This iron-dependent form of cell death can bypass classical apoptotic defects by leveraging lipid peroxidation to eradicate resistant cancer cells. Consequently, the development of Pt-based agents designed to trigger ferroptosis provides a viable alternative to overcome intrinsic and acquired chemoresistance, thereby expanding the therapeutic utility of Pt-based chemotherapeutics.

The rapid proliferation and resistance to apoptosis in cancer cells drive them into a state of heightened lipid and iron metabolism. This creates a metabolic vulnerability, paradoxically setting the stage for effective tumor eradication *via* ferroptosis.[114] Therefore, PSs capable of inducing ferroptosis are of great interest for combating apoptosis-resistant tumors.[115–117] Guo, He, and Chen *et al.* developed TTC-Pt (complex **7**, Fig. 12), a monofunctional Pt(II) complex exhibiting aggregation-induced emission (AIE) activity. The incorporation of Pt(II) into the TTC framework enhanced intersystem crossing (ISC), substantially boosting singlet oxygen production upon photoactivation.[118] TTC-Pt exhibited potent photoinduced growth inhibition against HeLa cells, with an IC_{50} of 0.34 ± 0.05 μM, significantly surpassing its precursor TTC (IC_{50} > 64.00 μM) and cisplatin (IC_{50} = 25.28 ± 1.32 μM), and showed negligible dark toxicity. Mechanistic investigations using specific inhibitors revealed that TTC-Pt-mediated PDT primarily induced ferroptosis and necroptosis, as evidenced by the inhibition of ferroptosis with ferrostatin-1 and the inhibition of necroptosis with necrostatin-1, rather than apoptosis or autophagy. Localized to lysosomes, TTC-Pt triggered ferroptosis *via* lipid peroxide accumulation and selectively downregulated FSP1 expression after irradiation, without altering GPX4 levels. This mechanism delineates a non-canonical pathway for ferroptosis induction driven by FSP1 suppression rather than GPX4 inhibition, likely resulting from TTC-Pt-induced disruption of cellular redox homeostasis. The concurrent induction of ferroptosis and necroptosis establishes a dual-mechanism strategy to effectively eliminate apoptosis-resistant tumor cells, offering a promising approach to circumventing chemotherapeutic resistance.

The aggregation of PSs often quenches ROS generation, thereby limiting their efficacy in PDT.[119–121] To overcome this challenge and advance PDT applications, particularly in combating drug resistance, high-performance PSs operable under physiological conditions are essential. Yuan and Hu *et al.* developed two Pt-based PSs, complexes **8** and **9** (Fig. 13), which bind to biomacromolecules to mitigate aggregation-caused quenching and enhance photosensitizing efficacy in biologically relevant environments.[122] Incorporating abundant heteroatoms into the Pt framework conferred these complexes a strong binding affinity for biological macromolecules. Upon confinement within bovine serum albumin (BSA), the molecular motion of the complexes became restricted, thereby

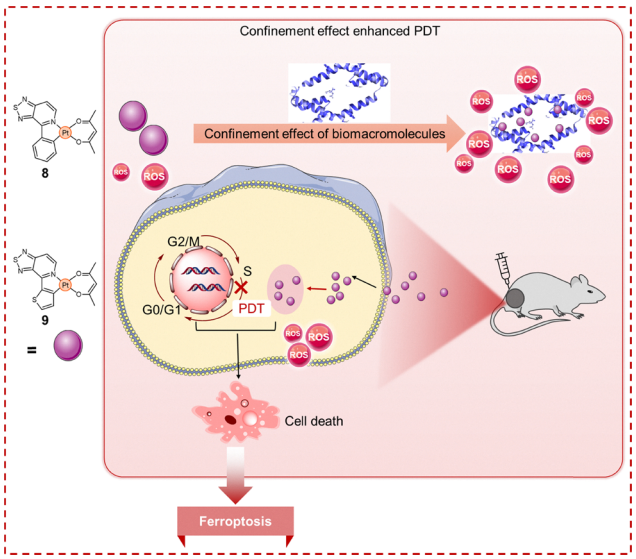

Fig. 13 Chemical structures of Pt(II) complexes **8** and **9** and the proposed mechanism of ferroptosis induced by complex **9**. The complex demonstrates high affinity for cellular biomacromolecules, whose constrained environment potentiates the production of cytotoxic ROS. The resulting oxidative stress cascade specifically induces ferroptosis, a mechanism responsible for the observed eradication of tumor cells in both cellular and animal models.

promoting the involvement of the central metal in excited-state charge transfer. This significantly boosted ROS generation, yielding a 2–3-fold increase in ROS production for BSA-bound complexes compared to free agents. The complexes exhibited dark cytotoxicity (IC_{50} = 6 μM), likely due to biomacromolecule binding. Upon white light irradiation, cytotoxicity was markedly enhanced (IC_{50}: complex **8** = 2.72 μM and complex **9** = 0.88 μM). This enhancement correlated with light-dependent BSA degradation (remaining percentages: 58.38% for complex **8** and 45.48% for complex **9**) and elevated intracellular ROS and oxidative stress. Cell death pathway analysis using specific inhibitors—ferrostatin-1 (Fer-1) for ferroptosis, Z-VAD-FMK for apoptosis, and VX-765 for pyroptosis—revealed that ferroptosis inhibition substantially abrogated cytotoxicity, identifying ferroptosis as the primary PDT pathway. The induction of ferroptosis may circumvent conventional apoptotic signaling and its associated resistance mechanisms. This feature renders ferroptosis a promising therapeutic strategy for combating drug-resistant malignancies, though further investigation is warranted. Notably, complex **9** demonstrated superior biocompatibility and tumor eradication efficacy *in vivo*, achieving significant tumor growth inhibition post-irradiation compared to controls. This work establishes the approach of leveraging Pt(II)–biomacromolecule interactions to develop potent PSs for ferroptosis-mediated PDT, which show considerable potential in overcoming chemoresistance limitations.

Ferrocene, initially explored in conjugates with tamoxifen and chloroquine, has become a valuable moiety in drug design.[123,124] Building on this concept, Sadler, Sicilia, and colleagues developed a ferrocene-conjugated Pt(IV) complex,

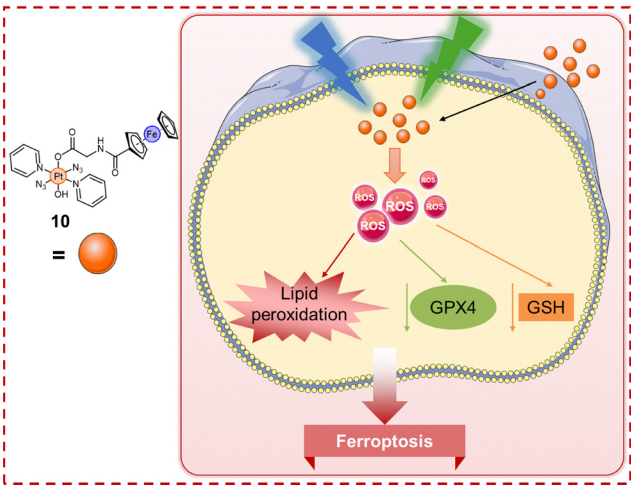

Fig. 14 Chemical structure and mechanism of action of complex **10**. Upon irradiation with blue or green light, complex **10** generates a high yield of ROS, which induce ferroptosis and thereby contribute to the execution of cell death.

Pt–Fe (complex **10**, Fig. 14), by appending the photoactive *trans*,*trans*,*trans*-$[Pt(N_3)_2(OH)_2(py)_2]$ to a ferrocene unit.[125] The ferrocene antenna red shifts the absorption profile, enabling Fe → Pt charge transfer and photoactivation at longer wavelengths. Upon 465 nm irradiation, complex **10** exhibited potent photocytotoxicity in A2780 ovarian cancer cells under both normoxia (IC_{50} = 0.8 ± 0.2 μM) and hypoxia (IC_{50} = 1.3 ± 0.3 μM), with comparable activity in cisplatin-resistant A2780cisR cells (normoxia: 1.4 ± 0.5 μM; hypoxia: 1.0 ± 0.1 μM), yielding RFs of 1.8 (normoxia) and 0.8 (hypoxia). In contrast, cisplatin under identical conditions showed only modest activity in A2780 cells (normoxia: 0.9 ± 0.5 μM; hypoxia: 8.8 ± 1 μM) and markedly reduced efficacy in A2780cisR cells (normoxia: 7.67 ± 0.04 μM; hypoxia: 16.2 ± 1.0 μM), with RFs of 8.5 (normoxia) and 1.8 (hypoxia), underscoring complex **10**'s ability to overcome resistance to both cisplatin and hypoxia. Mechanistically, photoactivated complex **10** markedly elevated ROS levels *via* ferrocene-mediated Fenton-type catalysis and induced lipid peroxidation, along with approximately 50% GSH depletion and approximately 60% suppression of GPX4. These hallmarks indicate ferroptosis as the primary cell death pathway, distinguishing complex **10** from conventional Pt(II) drugs and typical PSs. Collectively, the intermetallic charge-transfer design, robust photocytotoxicity, resilience to resistance, and ferroptosis induction position complex **10** as a promising photochemotherapeutic prodrug and a blueprint for the next-generation phototherapeutic agents.

5. Pt phototherapeutics that induce pyroptosis

Pyroptosis is an immunogenic form of lytic, programmed cell death characterized by hallmark morphological alterations, such as cell swelling, plasma membrane pore formation,

membrane rupture, and chromatin fragmentation.[126,127] This process has garnered significant attention due to its critical role in immunity and its potential applications in cancer therapy. Pyroptosis is primarily executed through canonical and non-canonical pathways, both of which converge on GSDMD cleavage (Fig. 15).[128–130] The canonical pathway is initiated by inflammasomes, which are multiprotein complexes (comprising pattern recognition receptors and adaptors such as ASC) that assemble in response to stimuli, such as pathogens, hypoxia, and damage-associated molecular patterns (DAMPs). Upon activation, inflammasomes catalyze the maturation of procaspase-1 into caspase-1; the latter subsequently cleaves both pro-interleukin-1β (pro-IL-1β) and pro-IL-18 into their bioactive forms while also cleaving GSDMD. The liberated GSDMD N-terminal domain oligomerizes in the plasma membrane, forming pores that induce lytic cell death and facilitate the extracellular release of potent inflammatory cytokines, particularly IL-1β and IL-18. This cytokine release can effectively reprogram the tumor microenvironment (TME), mitigating immunosuppression to convert immunologically "cold" tumors into "hot" phenotypes, thereby enhancing antitumor immunity.[131,132] The non-canonical pathway is primarily activated by Gram-negative bacterial lipopolysaccharide (LPS), which directly activates caspase-4/5 in humans (or caspase-11 in mice) to cleave GSDMD, initiating pyroptosis independent of inflammasomes. However, the non-canonical pathway lacks the capacity to process pro-IL-1β and pro-IL-18. Notably, pyroptosis can propagate through a mechanism in which extracellular vesicles containing GSDMD pore-forming structures, released from pyroptotic donor cells, integrate into the membrane of bystander cells, thereby triggering a cascade of pyroptosis.[133] This domino-like amplification of inflammatory signaling and immune activation holds significant therapeutic potential and could overcome limitations of traditional treatments, such as apoptosis-driven immune evasion and apoptosis-related drug resistance. Therefore, the development of Pt-based agents designed to elicit pyroptosis provides a viable therapeutic approach to overcoming chemoresistance and enhancing treatment efficacy in refractory malignancies.

The activation of the cGAS-STING pathway, a promising anticancer immunotherapeutic strategy, can be effectively achieved through photo-induced pyroptosis.[131,134–136] Previous work has established the biological applications of triphenylamine derivatives.[137,138] On this basis, Mao, Tan, and colleagues developed two novel small-molecule photoactivators, complexes **11** and **12** (Fig. 16), to target the cGAS-STING pathway and induce pyroptosis.[139] These Pt(II) complexes are structural analogues of cisplatin and transplatin, respectively, and incorporate an alkylated triphenylamine ligand. Complexes **11** and **12** exhibited negligible dark cytotoxicity (IC_{50} > 200 μM) across multiple cancer cell lines (HeLa, MDA-MB-231, A549, and U14). However, under 425 nm light irradiation, both complexes demonstrated significant photocytotoxicity, with the PI ranging from 17 to 106. Complex **11** displayed higher photocytotoxicity overall, with HeLa and U14 cells being particularly sensitive, as demonstrated by PIs of 79 and 106, respectively. In contrast, neither cisplatin nor transplatin showed any photocytotoxicity

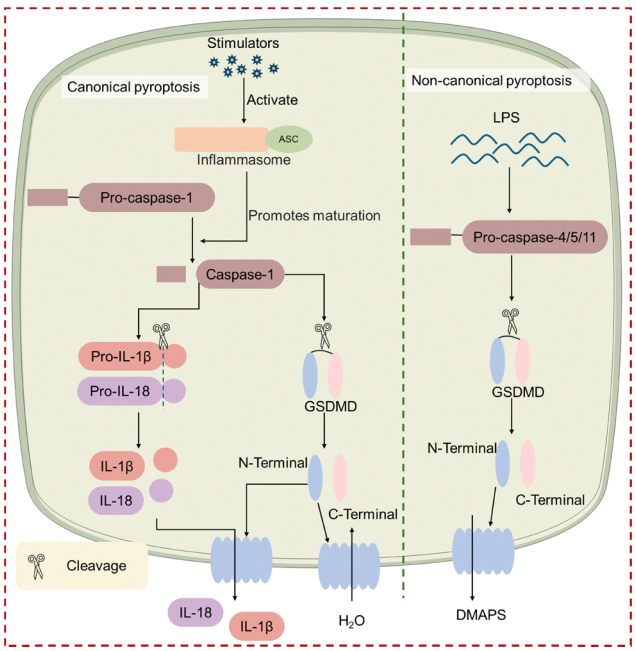

Fig. 15 Canonical and non-canonical pyroptosis pathways. Pyroptosis is an inflammatory form of lytic cell death. The canonical pathway is initiated by inflammasomes, which activate caspase-1 to cleave pro-interleukins into their mature forms and cleave gasdermin D (GSDMD). The N-terminal fragment of GSDMD oligomerizes to form plasma membrane pores, leading to cytokine release and cell lysis. In the non-canonical pathway, cytosolic lipopolysaccharide (LPS) directly activates human caspase-4/5 or murine caspase-11, which then cleaves GSDMD to induce pore formation and pyroptosis independent of inflammasomes.

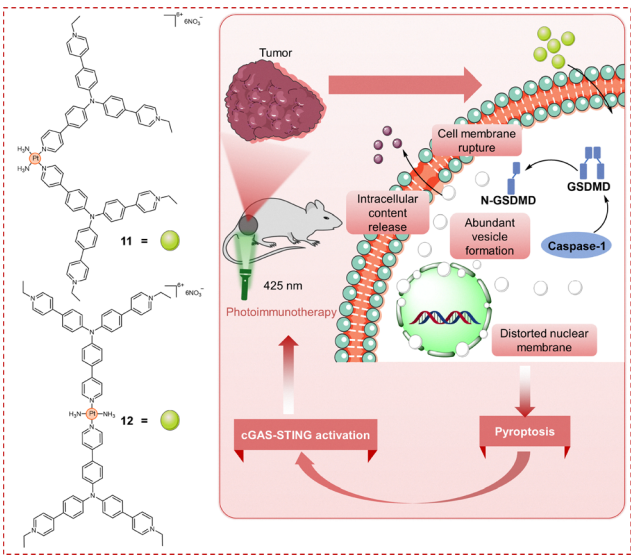

Fig. 16 Chemical structures and mechanism of action for complexes **11** and **12**. Upon photoactivation, these agents cause damage to DNA and the nuclear envelope, inducing pyroptotic cell death and activating the cGAS-STING pathway (cyclic GMP–AMP synthase–stimulator of interferon genes), which collectively stimulates an anticancer immune response *in vitro* and *in vivo*.

under identical conditions. PDT mediated by complexes **11** and **12** elicited pyroptosis, which was thoroughly confirmed through multiple lines of evidence. Transmission electron microscopy (TEM) of irradiated HeLa cells treated with complexes **11** or **12** revealed the characteristic pyroptotic morphology: cell membrane rupture, abundant vesicle formation, intracellular content release, and distorted nuclear membranes—observations further corroborated by confocal microscopy. In contrast, unirradiated controls displayed no such alterations. Inhibitor studies reinforced these findings; cell death was reduced by necrostatin-1 (a necroptosis inhibitor) and more significantly suppressed by necrosulfonamide (NSA; a necroptosis/pyroptosis inhibitor). Conversely, inhibitors of autophagy (3-methyladenine and chloroquine) or pan-caspase activity (Z-VAD-FMK) had minimal effects. Furthermore, western blotting detected a significant increase in GSDMD-N expression, the pyroptosis executioner protein responsible for plasma membrane pore formation, following photoactivation of the complexes. Thus, integrated morphological assessment, pharmacological inhibition, and biochemical detection unequivocally demonstrated that these complexes induce pyroptotic cell death. Moreover, light activation of these complexes sequentially caused damage to mitochondrial DNA (mtDNA), the nuclear envelope, and nuclear DNA—including G-quadruplex structures and double-stranded DNA. This cascade of genomic stress activated the cGAS-STING pathway. Along with the concomitant induction of pyroptosis, this dual activation elicited potent antitumor immune responses. Beyond their potent cellular effects, photoactivated complexes **11** and **12** significantly inhibited tumor growth in animal models. This was accompanied by the release of the 2′,3′-cyclic GMP-AMP (cGAMP) and cytokines, enhanced infiltration of $CD8^+/CD4^+$ T cells, and promotion of dendritic cell maturation. This study thereby pioneers small-molecule STING photoactivators and demonstrates that coupling their targeted activation with pyroptosis induction offers a strategic, dual-pronged approach to developing novel immunotherapeutics capable of overcoming resistance.

Photoactivated Pt(IV) prodrugs derived from clinical Pt(II) agents have drawn significant interest and typically employ O-donor axial ligands as the photosensitive components.[140] In contrast, N-donor ligands, especially N-heteroaromatics, offer a compelling alternative by promoting ligand-to-metal charge transfer (LMCT) and thereby enhancing Pt(IV) photoreactivity.[141,142] Very recently, our group developed two green-light-activatable carboplatin-based Pt(IV) prodrugs, flavoplatins **13** and **14** (Fig. 17), which incorporate flavonol derivatives as axial N-donor ligands.[143] These prodrugs undergo rapid photoreduction to release the active Pt(II) species together with the axial ligands. Upon green-light irradiation, flavoplatin **13** exhibited IC_{50} values of 18.3 ± 4.8 μM and 14.2 ± 4.2 μM in A2780 and A2780cisR cells, respectively, with an RF of 0.8, while flavoplatin **14** achieved IC_{50} values of 15.1 ± 0.7 μM and 15.6 ± 4.5 μM in the same cell lines, corresponding to an RF of 1.0. By comparison, carboplatin's photocytotoxicity in both cell lines exceeded 500 μM, indicating at least a 27-fold potency

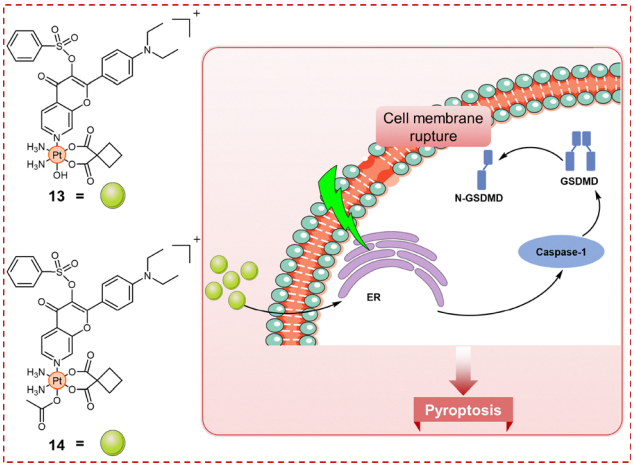

Fig. 17 Chemical structures and mechanism of action for complexes **13** and **14**. Upon irradiation with green light, complexes **13** and **14** localize to the endoplasmic reticulum (ER) and promptly elicit the NLRP3/caspase-1/GSDMD pyroptotic cell death.

advantage for both flavoplatins. Mechanistically, both complexes preferentially accumulated in the ER and promptly induced pyroptosis *via* the NLRP3/caspase-1/GSDMD pathway. This was evidenced by elevated NLRP3 expression, reduced procaspase-1 levels (by 39% for **13** and 28% for **14**), and a >3-fold increase in GSDMD N-terminal fragment, accompanied by a 26% decrease in full-length GSDMD for **13** in treated A2780cisR cells. These results confirm that light-activated flavoplatins can trigger pyroptosis in A2780cisR cells, a mechanism distinct from the apoptosis typically induced by conventional Pt(II) drugs, thereby offering a potential strategy to circumvent platinum resistance. Collectively, these findings highlight the therapeutic potential of Pt(IV) prodrugs bearing axial N-donor ligands, particularly their ability to engage non-apoptotic cell death pathways to mitigate drug resistance.

6. Pt phototherapeutics that induce ICD

ICD, a form of PCD defined by the NCCD as capable of eliciting adaptive immunity in immunocompetent hosts, was first identified in 2005 by Kroemer *et al.* based on their observation that anthracycline-treated tumor cells can provoke adjuvant-free immune responses.[41,144] This stress-induced process stimulates inflammatory responses that activate cytotoxic T lymphocyte (CTL)-mediated adaptive immunity and establishes long-lasting immunological memory, thereby gaining significant research interest in recent years.[53,145,146] The induction of ICD is characterized by several biochemical hallmarks (Fig. 18): (i) during early apoptosis, endoplasmic reticulum (ER)-resident calreticulin (endo-CRT) translocates to the plasma membrane (ecto-CRT), where it functions as an "eat me" signal by binding to the CD91 receptor on immature dendritic cells (DCs) and macrophages, thereby promoting phagocytosis; (ii) dying cells actively secrete ATP, which serves

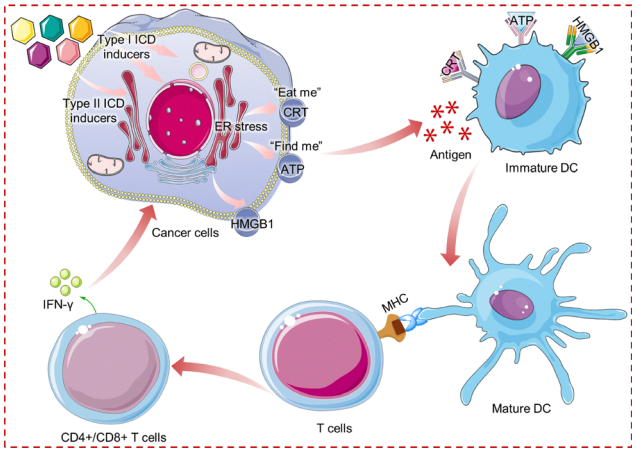

Fig. 18 Mechanism of ICD and subsequent activation of the immune response. ICD inducers trigger endoplasmic reticulum (ER) stress in cancer cells through direct (type II) or indirect (type I) pathways, culminating in ICD. Dying cells release damage-associated molecular patterns (DAMPs), including surface-exposed calreticulin (ecto-CRT), which acts as an "eat me" signal for phagocytosis, secreted adenosine triphosphate (ATP) and released high mobility group box 1 (HMGB1), which serve as "find me" signals. DAMPs attract immune cells to the ICD site and engage with specific receptors on antigen-presenting cells (APCs), enhancing antigen uptake and processing. Subsequently, mature APCs present tumor antigens to T cells, leading to the priming of tumor-specific $CD8^+$ T cells that secrete interferon-gamma (IFN-γ), which promotes tumor cell elimination.

as a "find me" signal to attract antigen-presenting cells *via* P2RX7 receptor binding; and (iii) during late apoptosis, membrane damage facilitates the release of the nuclear protein HMGB1 into the extracellular space, further enhancing immunogenicity.[147–149] Crucially, the simultaneous occurrence of CRT exposure, ATP secretion, and HMGB1 release is essential for ICD efficacy. The absence or neutralization of any single hallmark abrogates immunogenicity, compromising the effectiveness of immunochemotherapy.[150,151] ER stress is a pivotal trigger for ICD, with ICD inducers classified as type I (*e.g.*, mitoxantrone, doxorubicin, and oxaliplatin) or type II (*e.g.*, coxsackievirus B3, hypericin, and oncolytic viruses) according to their ER targeting specificity.[149,152,153] Type I inducers act on diverse cellular compartments and indirectly provoke ER stress and DAMP release through secondary effects. In contrast, type II inducers primarily localize within the ER, directly disrupting its homeostasis *via* oxidative stress, an action that facilitates ICD.[154] Type II inducers are thought to elicit a stronger ICD immune response due to their capacity for generating higher DAMP levels.[147] The immunogenicity of ICD ultimately arises from the release of DAMPs, which signal through pattern recognition receptors (PRRs) on antigen-presenting cells (APCs). This interaction orchestrates the uptake and presentation of tumor antigens, culminating in APC activation and the priming of tumor-specific T cells. These effector T cells subsequently infiltrate and eliminate malignant cells. The strategic development of Pt-based ICD inducers exemplifies a promising approach to overcoming conventional drug resistance. Unlike cisplatin, which induces immunologically silent apoptosis, ICD inducers emit a suite of danger signals that activate dendritic cells and prime a cytotoxic T cell response. This mechanism effectively recruits the host's immune system to eradicate both primary and metastatic cancer cells, thus bypassing intrinsic resistance mechanisms and potentially conferring durable, systemic protection against relapse.

Photoactivatable Pt(IV) complexes represent compelling candidates for overcoming Pt resistance through a mechanism of action distinct from that of cisplatin. A prime example is *trans*,*trans*,*trans*-$[Pt(N_3)_2(OH)_2(py)_2]$ (complex **15**, Fig. 19), a stable and non-toxic prodrug in the dark that becomes highly cytotoxic upon UVA/visible light irradiation.[155] Upon photoactivation, complex **15** generates reactive Pt(II) species that target DNA, while simultaneously releasing ROS and reactive nitrogen species (RNS). These species collectively elevate intracellular oxidative stress and promote the induction of ICD. Photoactivated complex **15** (at 1 or 5 μM), unlike cisplatin (at 20 μM), induced significant ecto-CRT exposure in A2780 ovarian cancer cells upon irradiation, as confirmed by flow cytometry and confocal microscopy. This response was comparable to that of established ICD inducers such as doxorubicin (at 20 μM) and oxaliplatin (at 100 μM). Furthermore, photoactivated complex **15**, together with doxorubicin and oxaliplatin, stimulated the release of the key ICD biomarkers HMGB1 and ATP from A2780 cells in a concentration-dependent manner. In contrast, untreated cells, cisplatin, or complex **15** in the dark failed to elicit these biomarkers. Crucially, photoactivated complex **15** uniquely promoted efficient phagocytosis of murine CT26 carcinoma cells by J774-A1 macrophages (35.1 ± 5.6%), significantly outperforming both complex **15** in the dark (2.8 ± 0.4%) and untreated controls (2.4 ± 0.2%). Remarkably, oxaliplatin (100 μM), despite inducing ecto-CRT and ICD biomarkers, did not elicit comparable phagocytosis, and cisplatin (20 μM) showed negligible activity. This dual ability to induce ICD biomarkers and potent phagocytosis reveals a new mechanism of action for complex **15**, highlighting its potential to circumvent Pt resistance by eliciting robust antitumor immunity.

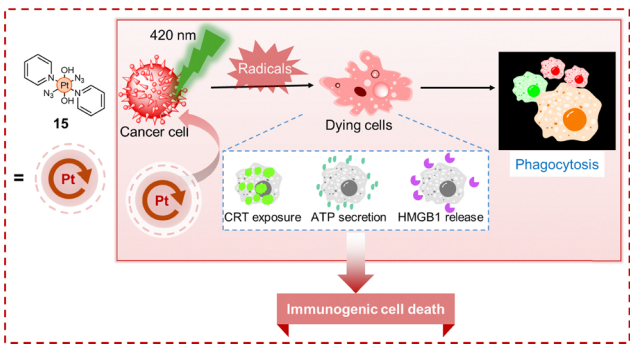

Fig. 19 Structure and mechanism of photoactivatable Pt(IV) prodrug **15**. Visible light irradiation decomposes **15**, releasing cytotoxic Pt(II) species and generating reactive oxygen/nitrogen species (ROS and RNS). This dual action induces ICD, evidenced by CRT exposure, HMGB1 release, ATP secretion, and subsequent phagocytosis. This ICD mechanism differentiates **15** from conventional Pt agents and offers a potential strategy to circumvent Pt resistance.

Light-triggered ICD inducers remain rare, positioning photoactivatable Pt complexes as compelling candidates. Rationally designed photocaged Pt(IV) prodrugs enable spatiotemporally controlled activation, minimizing off-target effects while potentially eliciting ICD-mediated antitumor immunity. Motivated by this potential, our group developed coumaplatin (complex **16**, Fig. 20), an oxaliplatin-derived prodrug functionalized with a photocaging coumarin moiety and a nuclear localization sequence (R_8K) for nucleolus targeting.[156] Coumaplatin exhibited exceptional stability in the dark and rapid photoactivation within cells. Upon irradiation, it significantly outperformed oxaliplatin, demonstrating a more than 2-fold increase in DNA binding efficiency and up to 96-fold enhanced phototoxicity. Additionally, coumaplatin exhibited a superior ability to circumvent Pt resistance. In Pt-resistant A2780cisR and A549cisR cells, oxaliplatin displayed RFs of 5.1 and 2.8, respectively, while photoactivated coumaplatin markedly reduced these RFs to 1.3 and 0.6. Critically, photoactivated coumaplatin—unlike oxaliplatin or its inactive form of coumaplatin—induced ICD-associated DAMPs in resistant cells. Specifically, it significantly induced CRT exposure on A549cisR cell membranes, as confirmed by both microscopy and flow cytometry. Furthermore, photoactivated coumaplatin triggered HMGB1 translocation from the nucleus to the cytoplasm and significantly increased extracellular ATP secretion (56.7 nM *versus* 35.9 nM with oxaliplatin). Notably, low-dose photoactivated coumaplatin elicited ICD and robust T cell activation in resistant cells, effects that are unattainable even with high-dose oxaliplatin. By leveraging nucleolus-targeted photoactivation, coumaplatin uniquely induced potent ICD and profoundly overcame Pt resistance, heralding a paradigm shift for light-triggered antitumor immunity.

Cancer immunotherapy, while transformative, is often undermined by tumor immune evasion *via* downregulation of major histocompatibility complex class I (MHC-I).[157,158] To address this challenge, Guo, Mao, and colleagues rationally designed a trinuclear Ru–Pt complex, TriRuPt (complex **17**,

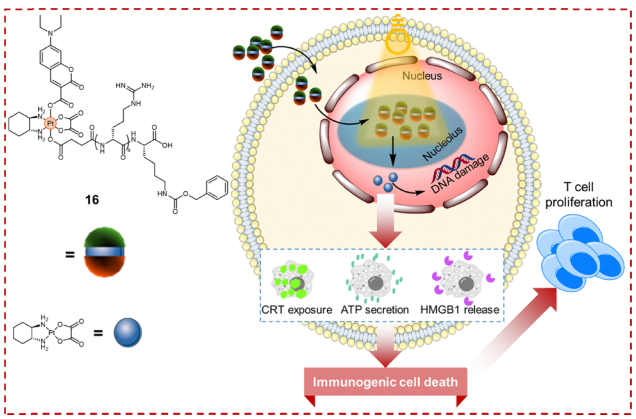

Fig. 20 Chemical structure and mechanism of action for complex **16**. Upon cellular accumulation in the nucleolus and subsequent photoactivation, complex **16** initiates immunogenic cell death and activates T cells, providing a mechanism to overcome conventional Pt drug resistance.

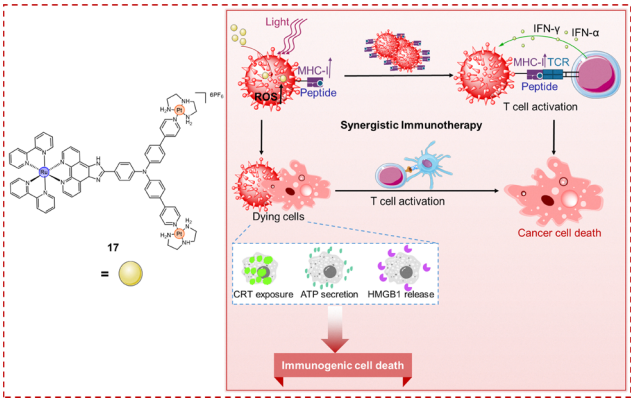

Fig. 21 Chemical structure and mechanism of action for complex **17**. Complex **17** as a PS in PDT generates ROS that disrupt cellular homeostasis and elicits two immunomodulatory effects: (i) upregulation of major histocompatibility complex class I (MHC-I) to enhance T cell recognition and activation and (ii) induction of ICD, promoting dendritic cell-mediated antigen presentation and amplified antitumor immunity.

Fig. 21), which leverages the photophysical properties of transition metals to modulate MHC-I expression.[159] Complex **17** demonstrated superior light-triggered cytotoxicity compared to cisplatin, effectively overcoming drug resistance, as demonstrated by IC_{50} values of 0.144 μM in human lung adenocarcinoma A549 cells and 0.245 μM in cisplatin-resistant A549cisR cells, yielding a PI exceeding 100 and an RF of 1.7. In contrast, cisplatin exhibited IC_{50} values of 2.74 μM (A549) and 12.0 μM (A549cisR), with an RF of 4.4. Mechanistically, complex **17** functions as a PS to generate ROS, initiating a dual immunomodulatory cascade: (1) light-driven upregulation of MHC-I, which promotes T cell recognition and activation, and (2) induction of ICD, characterized by release of DAMPs such as HMGB1, cell-membrane exposure of CRT, and elevated ATP secretion, thereby enhancing dendritic cell-mediated antigen presentation and amplifying T cell responses. Through this dual mechanism, complex **17** converts immune-"cold" tumors to immune-"hot" phenotypes and acts synergistically with immune checkpoint inhibitors (ICIs) *in vivo*, resulting in suppressed tumor growth, reprogramming of the tumor microenvironment, and enhanced adaptive immunity. Overall, this metal-mediated PDT approach simultaneously elevates MHC-I levels and triggers ICD to enhance ICI therapy, uncovering a novel immunoregulatory function of transition metal complexes and paving the way for metal-based strategies to circumvent tumor immune evasion and resistance *via* integrated immunomodulation.

7. Conclusions and future perspectives

Conventional Pt-based chemotherapeutics induce cytotoxicity primarily by inhibiting proliferation and triggering apoptosis. However, their efficacy is often compromised by intrinsic or acquired resistance, frequently resulting from defects within apoptotic signaling cascades. In contrast, photoactivatable Pt complexes represent a transformative strategy, leveraging the

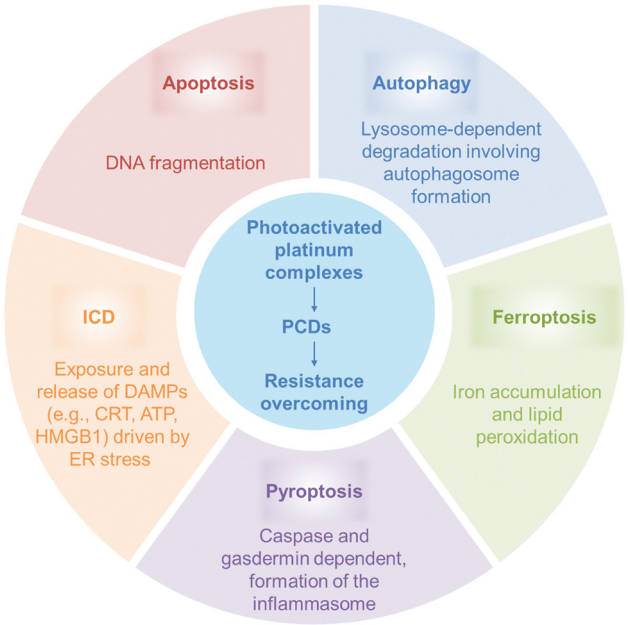

Fig. 22 Expanding the cell death repertoire: a schematic of the biochemical features of diverse programmed cell death pathways induced by photoactivated Pt complexes to circumvent drug resistance.

light-triggered generation of reactive Pt species and/or radicals that target cellular components independent of classical Pt–DNA adduct formation, thereby effectively bypassing canonical resistance mechanisms. By either potentiating apoptosis or engaging alternative PCD modalities, including autophagy, ferroptosis, pyroptosis, and ICD (Fig. 22), these agents dismantle tumor defenses through the combined actions of photo-induced species. For example, autophagy can proceed despite defects in apoptosis, providing an alternative degradation route. Ferroptosis, driven by iron-dependent lipid peroxidation or inhibition of ferroptosis suppressor protein 1, eliminates cells refractory to apoptosis. Pyroptosis, initiated *via* inflammasome activation and subsequent gasdermin-mediated pore formation, induces direct lytic death while provoking robust inflammatory responses that synergize with immunotherapy. ICD converts immunologically "cold" tumors into "hot" ones by promoting dendritic cell maturation and cytotoxic T lymphocyte infiltration. Collectively, photoactivatable Pt complexes that trigger diverse cell death pathways provide a versatile, spatiotemporally precise approach to re-sensitizing resistant tumors and improving therapeutic outcomes (Table 1).

Future advancements in phototherapeutic Pt complexes necessitate a strategic shift from primarily inducing apoptosis toward the deliberate engagement of non-apoptotic PCD pathways, particularly ICD and pyroptosis, which uniquely leverage antitumor immunity to counteract immunosuppressive microenvironments. A major bottleneck remains the lack of predictive design principles; the activation of these pathways in current photoactivatable Pt complexes is largely discovered through serendipity. Emerging studies have begun to identify actionable targets that trigger non-apoptotic PCD, such as

Table 1 Summary of the representative Pt complexes: mechanisms, key markers, and resistance-bypassing advantages

PCD	Representative Pt complex	Mechanism	Key marker	Resistance-bypassing advantage	Ref.
Apoptosis	Complex **2** (irradiated at 480/595 nm)	Photoactivated shift to caspase-mediated apoptosis	Increased caspase 3/7 activity under irradiation	Overcomes resistance; low RFs[a] (1.06–1.25 in A2780cisR/A2780 and A2780ADR/A2780) *vs.* cisplatin (RFs: 1.98–4.30)	74
Autophagy	Complex **6** (UVA-activated)	UVA-activated autophagic flux	Increased LC3B-II; decreased p62	Overcome resistance; low RFs (0.88–1.20) *vs.* cisplatin (RFs: 2.07–2.89) in resistant cell lines	99
Ferroptosis	Complex **10** (465 nm-irradiated)	Photoactivated ROS elevation *via* Fenton catalysis, leading to lipid peroxidation and antioxidant depletion	Elevated ROS; lipid peroxidation; ~50% GSH depletion; ~60% GPX4 reduction	Bypasses cisplatin and hypoxia resistance; RFs 0.8–1.8 (normoxia/hypoxia) in A2780cisR/A2780 *vs.* cisplatin 1.8–8.5	125
Pyroptosis	Flavoplatin **13** (green light-activated)	ER-targeted activation of the NLRP3/caspase-1/GSDMD pathway	Elevated NLRP3; reduced pro-caspase-1; >3-fold increased GSDMD-NT; 26% decreased full-length GSDMD	Circumvents cisplatin resistance with an RF of 0.in A2780cisR/A2780 cells; ≥27-fold more photocytotoxic than carboplatin	143
Immunogenic cell death (ICD)	Complex **16** (visible light 450 nm-irradiated)	Photoactivated DAMP exposure triggering the immune response	CRT membrane exposure; HMGB1 nuclear-to-cytoplasmic translocation; extracellular ATP secretion	Circumvents Pt resistance; RFs 0.6–1.3 in A2780cisR/A549cisR *vs.* oxaliplatin 2.8–5.1	156

[a] RF (resistance factor) = IC_{50} (platinum-resistant cell line)/IC_{50} (platinum-sensitive cell line).

mTOR inhibition for autophagy-dependent cell death, GPX4 inhibition for ferroptosis, ER stress for ICD, and GSDMD cleavage for pyroptosis, pointing to opportunities for rational design. Beyond these, additional forms of cell death—such as disulfidptosis, oncosis, paraptosis, necroptosis, necrosis, and parthanatos—represent further frontiers. The rational design of Pt phototherapeutics to modulate these targets may open new avenues to overcome resistance. Moreover, the strategic induction of multi-pathway cell death, potentially *via* combinatorial approaches, offers a powerful means to circumvent single-agent resistance and improve therapeutic outcomes. In parallel, deep learning (DL) can help predict multifaceted cytotoxic profiles in cases where structure–activity relationships (SARs) are unclear, but its success depends on large-scale, high-quality datasets; therefore, high-throughput synthesis, screening, and evaluation of photoactivatable Pt complexes will be essential to generate robust training data.

Equally critical is the transition to physiologically relevant preclinical models. Many resistance studies still rely on monolayer cultures that do not adequately recapitulate tumor architecture, hypoxia gradients, and stromal interactions. Patient-derived organoids and tumoroids preserve native 3D organization, genetic heterogeneity, and microenvironmental fidelity, providing more predictive platforms to evaluate whether phototherapeutic Pt agents can overcome clinically relevant resistance mechanisms. In addition, tissue penetration by light is strongly wavelength-dependent, with NIR (700–900 nm) light achieving substantially deeper penetration and reduced off-target phototoxicity, thereby enhancing clinical translatability. Accordingly, future efforts should prioritize the rational design and development of NIR-activatable Pt complexes.

In summary, photoactivatable Pt complexes represent a transformative leap forward in overcoming Pt resistance by redirecting cytotoxicity from conventional DNA damage-driven apoptosis toward multimodal, immunity-engaging regulated cell death modalities. By orchestrating diverse PCD pathways with spatiotemporal control, phototherapeutic Pt agents offer robust solutions to chemoresistance and lay the groundwork for next-generation precision oncology therapeutics.

Author contributions

The manuscript was written through contributions of S. C., Z. G., and G. Z. All authors have given approval to the final version of the manuscript.

Conflicts of interest

The authors declare no conflicts of interest.

Data availability

No primary research results, software or code have been included and no new data were generated or analysed as part of this review.

Acknowledgements

We thank the Hong Kong Research Grants Council (grant nos. CityU 11313222, CityU 11304923, CityU 11306724, and CityU C1018-23G), the National Natural Science Foundation of China (grant nos. 22277103 and 22525703), the Science Technology and Innovation Committee of Shenzhen Municipality (JCYJ20210324120004011), and the City University of Hong Kong (grant no. 7020014) for funding support. Parts of the scheme and figures were drawn using pictures from Servier Medical Art. Servier Medical Art by Servier is licensed under a Creative Commons Attribution 4.0 Unported License (https://creativecommons.org/licenses/by/4.0/).

References

1 L. Kelland, *Nat. Rev. Cancer*, 2007, **7**, 573–584.
2 B. W. Harper, A. M. Krause-Heuer, M. P. Grant, M. Manohar, K. B. Garbutcheon-Singh and J. R. Aldrich-Wright, *Chem. – Eur. J.*, 2010, **16**, 7064–7077.
3 N. J. Wheate, S. Walker, G. E. Craig and R. Oun, *Dalton Trans.*, 2010, **39**, 8113–8127.
4 T. C. Johnstone, K. Suntharalingam and S. J. Lippard, *Chem. Rev.*, 2016, **116**, 3436–3486.
5 M. D. Hall, H. R. Mellor, R. Callaghan and T. W. Hambley, *J. Med. Chem.*, 2007, **50**, 3403–3411.
6 S. Dilruba and G. V. Kalayda, *Cancer Chemother. Pharmacol.*, 2016, **77**, 1103–1124.
7 J. J. Roberts and A. J. Thomson, *Prog. Nucleic Acid Res. Mol. Biol.*, 1979, **22**, 71–133.
8 O. Pinato, C. Musetti and C. Sissi, *Metallomics*, 2014, **6**, 380–395.
9 E. R. Jamieson and S. J. Lippard, *Chem. Rev.*, 1999, **99**, 2467–2498.
10 S. W. G. Tait and D. R. Green, *Nat. Rev. Mol. Cell Biol.*, 2010, **11**, 621–632.
11 T. Boulikas and M. Vougiouka, *Oncol. Rep.*, 2003, **10**, 1663–1682.
12 D. Wang and S. J. Lippard, *Nat. Rev. Drug Discovery*, 2005, **4**, 307–320.
13 S. Dasari and P. B. Tchounwou, *Eur. J. Pharmacol.*, 2014, **740**, 364–378.
14 T. C. Johnstone, K. Suntharalingam and S. J. Lippard, *Philos. Trans. R. Soc., A*, 2015, **373**, 20140185.
15 K. D. Mjos and C. Orvig, *Chem. Rev.*, 2014, **114**, 4540–4563.
16 S. Rottenberg, C. Disler and P. Perego, *Nat. Rev. Cancer*, 2021, **21**, 37–50.
17 N. Nagai, R. Okuda, M. Kinoshita and H. Ogata, *J. Pharm. Pharmacol.*, 1996, **48**, 918–924.
18 E. J. Anthony, E. M. Bolitho, H. E. Bridgewater, O. W. L. Carter, J. M. Donnelly, C. Imberti, E. C. Lant, F. Lermyte, R. J. Needham, M. Palau, P. J. Sadler, H. Shi, F.-X. Wang, W.-Y. Zhang and Z. Zhang, *Chem. Sci.*, 2020, **11**, 12888–12917.
19 A. Casini and A. Pöthig, *ACS Cent. Sci.*, 2024, **10**, 242–250.
20 Y. Wang, B. Cao, Q. Wang, S. Zhong, X. Fang, J. Wang, A. S. C. Chan, X. Xiong and T. Zou, *Nat. Commun.*, 2025, **16**, 7347.
21 M. D. Coskun, F. Ari, A. Y. Oral, M. Sarimahmut, H. M. Kutlu, V. T. Yilmaz and E. Ulukaya, *Bioorg. Med. Chem.*, 2013, **21**, 4698–4705.
22 Ž. D. Bugarčić, J. Bogojeski and R. van Eldik, *Coord. Chem. Rev.*, 2015, **292**, 91–106.
23 T. Lazarević, A. Rilak and Ž. D. Bugarčić, *Eur. J. Med. Chem.*, 2017, **142**, 8–31.
24 I. Ott, *Coord. Chem. Rev.*, 2009, **253**, 1670–1681.
25 S. Nobili, E. Mini, I. Landini, C. Gabbiani, A. Casini and L. Messori, *Med. Res. Rev.*, 2010, **30**, 550–580.
26 C. S. Allardyce and P. J. Dyson, *Platinum Met. Rev.*, 2001, **45**, 62–69.
27 N. Muhammad and Z. Guo, *Curr. Opin. Chem. Biol.*, 2014, **19**, 144–153.
28 R. Oun, Y. E. Moussa and N. J. Wheate, *Dalton Trans.*, 2018, **47**, 6645–6653.

29 J. T. Hartmann and H.-P. Lipp, *Expert Opin. Pharmacother.*, 2003, **4**, 889–901.
30 Z. H. Siddik, *Oncogene*, 2003, **22**, 7265–7279.
31 A.-M. Florea and D. Büsselberg, *Cancers*, 2011, **3**, 1351–1371.
32 M. Ohmichi, J. Hayakawa, K. Tasaka, H. Kurachi and Y. Murata, *Trends Pharmacol. Sci.*, 2005, **26**, 113–116.
33 G. Giaccone, *Drugs*, 2000, **59**, 9–17.
34 J. Zhou, Y. Kang, L. Chen, H. Wang, J. Liu, S. Zeng and L. Yu, *Front. Pharmacol.*, 2020, **11**, 343.
35 V. Brabec and J. Kasparkova, *Drug Resistance Updates*, 2002, **5**, 147–161.
36 F. H. Igney and P. H. Krammer, *Nat. Rev. Cancer*, 2002, **2**, 277–288.
37 S. Elmore, *Toxicol. Pathol.*, 2007, **35**, 495–516.
38 E. V. Sazonova, G. S. Kopeina, E. N. Imyanitov and B. Zhivotovsky, *Cell Death Discovery*, 2021, **7**, 155.
39 U. Ziegler and P. Groscurth, *Physiology*, 2004, **19**, 124–128.
40 L. Galluzzi, M. C. Maiuri, I. Vitale, H. Zischka, M. Castedo, L. Zitvogel and G. Kroemer, *Cell Death Differ.*, 2007, **14**, 1237–1243.
41 L. Galluzzi, I. Vitale, S. A. Aaronson, J. M. Abrams, D. Adam, P. Agostinis, E. S. Alnemri, L. Altucci, I. Amelio, D. W. Andrews, M. Annicchiarico-Petruzzelli, A. V. Antonov, E. Arama, E. H. Baehrecke, N. A. Barlev, N. G. Bazan, F. Bernassola, M. J. M. Bertrand, K. Bianchi, M. V. Blagosklonny, K. Blomgren, C. Borner, P. Boya, C. Brenner, M. Campanella, E. Candi, D. Carmona-Gutierrez, F. Cecconi, F. K.-M. Chan, N. S. Chandel, E. H. Cheng, J. E. Chipuk, J. A. Cidlowski, A. Ciechanover, G. M. Cohen, M. Conrad, J. R. Cubillos-Ruiz, P. E. Czabotar, V. D'Angiolella, T. M. Dawson, V. L. Dawson, V. De Laurenzi, R. De Maria, K.-M. Debatin, R. J. DeBerardinis, M. Deshmukh, N. Di Daniele, F. Di Virgilio, V. M. Dixit, S. J. Dixon, C. S. Duckett, B. D. Dynlacht, W. S. El-Deiry, J. W. Elrod, G. M. Fimia, S. Fulda, A. J. García-Sáez, A. D. Garg, C. Garrido, E. Gavathiotis, P. Golstein, E. Gottlieb, D. R. Green, L. A. Greene, H. Gronemeyer, A. Gross, G. Hajnoczky, J. M. Hardwick, I. S. Harris, M. O. Hengartner, C. Hetz, H. Ichijo, M. Jäättelä, B. Joseph, P. J. Jost, P. P. Juin, W. J. Kaiser, M. Karin, T. Kaufmann, O. Kepp, A. Kimchi, R. N. Kitsis, D. J. Klionsky, R. A. Knight, S. Kumar, S. W. Lee, J. J. Lemasters, B. Levine, A. Linkermann, S. A. Lipton, R. A. Lockshin, C. López-Otín, S. W. Lowe, T. Luedde, E. Lugli, M. MacFarlane, F. Madeo, M. Malewicz, W. Malorni, G. Manic, J.-C. Marine, S. J. Martin, J.-C. Martinou, J. P. Medema, P. Mehlen, P. Meier, S. Melino, E. A. Miao, J. D. Molkentin, U. M. Moll, C. Muñoz-Pinedo, S. Nagata, G. Nuñez, A. Oberst, M. Oren, M. Overholtzer, M. Pagano, T. Panaretakis, M. Pasparakis, J. M. Penninger, D. M. Pereira, S. Pervaiz, M. E. Peter, M. Piacentini, P. Pinton, J. H. M. Prehn, H. Puthalakath, G. A. Rabinovich, M. Rehm, R. Rizzuto, C. M. P. Rodrigues, D. C. Rubinsztein, T. Rudel, K. M. Ryan, E. Sayan, L. Scorrano, F. Shao, Y. Shi, J. Silke, H.-U. Simon, A. Sistigu, B. R. Stockwell, A. Strasser, G. Szabadkai, S. W. G. Tait, D. Tang, N. Tavernarakis, A. Thorburn, Y. Tsujimoto, B. Turk, T. Vanden Berghe, P. Vandenabeele, M. G. Vander Heiden, A. Villunger, H. W. Virgin, K. H. Vousden, D. Vucic, E. F. Wagner, H. Walczak, D. Wallach, Y. Wang, J. A. Wells, W. Wood, J. Yuan, Z. Zakeri, B. Zhivotovsky, L. Zitvogel, G. Melino and G. Kroemer, *Cell Death Differ.*, 2018, **25**, 486–541.
42 D. Tang, R. Kang, T. V. Berghe, P. Vandenabeele and G. Kroemer, *Cell Res.*, 2019, **29**, 347–364.
43 F. Peng, M. Liao, R. Qin, S. Zhu, C. Peng, L. Fu, Y. Chen and B. Han, *Signal Transduction Targeted Ther.*, 2022, **7**, 286.
44 K. M. Kuznetsov, K. Cariou and G. Gasser, *Chem. Sci.*, 2024, **15**, 17760–17780.
45 H. Shi, R. C. Marchi and P. J. Sadler, *Angew. Chem., Int. Ed.*, 2025, **64**, e202423335.
46 Y. Zhang, C. Xu, X. Yang and K. Pu, *Adv. Mater.*, 2020, **32**, 2002661.
47 T. C. Pham, V.-N. Nguyen, Y. Choi, S. Lee and J. Yoon, *Chem. Rev.*, 2021, **121**, 13454–13619.
48 J.-J. Hu, Q. Lei and X.-Z. Zhang, *Prog. Mater. Sci.*, 2020, **114**, 100685.
49 K. Xiong, F. Wei, Y. Chen, L. Ji and H. Chao, *Small Methods*, 2023, **7**, 2201403.
50 M. Dichiara, O. Prezzavento, A. Marrazzo, V. Pittala, L. Salerno, A. Rescifina and E. Amata, *Eur. J. Med. Chem.*, 2017, **142**, 459–485.
51 A. P. Castano, T. N. Demidova and M. R. Hamblin, *Photodiagn. Photodyn. Ther.*, 2004, **1**, 279–293.
52 L. Duprez, E. Wirawan, T. Vanden Berghe and P. Vandenabeele, *Microbes Infect.*, 2009, **11**, 1050–1062.
53 K. Peng, Y. Zheng, W. Xia and Z.-W. Mao, *Chem. Soc. Rev.*, 2023, **52**, 2790–2832.
54 G. E. Villalpando-Rodriguez and S. B. Gibson, *Oxid. Med. Cell. Longevity*, 2021, **2021**, 9912436.
55 G. V. Putcha, C. A. Harris, K. L. Moulder, R. M. Easton, C. B. Thompson and E. M. Johnson Jr, *J. Cell Biol.*, 2002, **157**, 441–453.
56 N. Yan and Y. Shi, *Annu. Rev. Cell Dev. Biol.*, 2005, **21**, 35–56.
57 J. P. Sheridan, S. A. Marsters, R. M. Pitti, A. Gurney, M. Skubatch, D. Baldwin, L. Ramakrishnan, C. L. Gray, K. Baker, W. I. Wood, A. D. Goddard, P. Godowski and A. Ashkenazi, *Science*, 1997, **277**, 818–821.
58 M. Kist and D. Vucic, *EMBO J.*, 2021, **40**, e106700.
59 A. Ashkenazi and V. M. Dixit, *Science*, 1998, **281**, 1305–1308.
60 Q. Hu, D. Wu, W. Chen, Z. Yan, C. Yan, T. He, Q. Liang and Y. Shi, *Proc. Natl. Acad. Sci. U. S. A.*, 2014, **111**, 16254–16261.
61 S. J. Riedl and G. S. Salvesen, *Nat. Rev. Mol. Cell Biol.*, 2007, **8**, 405–413.
62 J. M. Schriewer, C. B. Peek, J. Bass and P. T. Schumacker, *J. Am. Heart Assoc.*, 2013, **2**, e000159.
63 T. Zhong, J. Yu, Y. Pan, N. Zhang, Y. Qi and Y. Huang, *Adv. Healthcare Mater.*, 2023, **12**, 2300253.
64 Y. Wu, S. Li, Y. Chen, W. He and Z. Guo, *Chem. Sci.*, 2022, **13**, 5085–5106.
65 Y. Wang, X. Shi, H. Fang, Z. Han, H. Yuan, Z. Zhu, L. Dong, Z. Guo and X. Wang, *J. Med. Chem.*, 2022, **65**, 7786–7798.
66 M. D. Hall and T. W. Hambley, *Coord. Chem. Rev.*, 2002, **232**, 49–67.
67 K. Suntharalingam, Y. Song and S. J. Lippard, *Chem. Commun.*, 2014, **50**, 2465–2468.
68 R. Ma, Y. Wang, L. Yan, L. Ma, Z. Wang, H. C. Chan, S.-K. Chiu, X. Chen and G. Zhu, *Chem. Commun.*, 2015, **51**, 7859–7862.
69 X. Wang, X. Wang, S. Jin, N. Muhammad and Z. Guo, *Chem. Rev.*, 2018, **119**, 1138–1192.
70 F. E. Poynton, S. A. Bright, S. Blasco, D. C. Williams, J. M. Kelly and T. Gunnlaugsson, *Chem. Soc. Rev.*, 2017, **46**, 7706–7756.
71 J. Liu, C. Zhang, T. W. Rees, L. Ke, L. Ji and H. Chao, *Coord. Chem. Rev.*, 2018, **363**, 17–28.
72 J. D. Knoll and C. Turro, *Coord. Chem. Rev.*, 2015, **282**, 110–126.
73 L. Ma, L. Li and G. Zhu, *Inorg. Chem. Front.*, 2022, **9**, 2424–2453.
74 J. Karges, T. Yempala, M. Tharaud, D. Gibson and G. Gasser, *Angew. Chem., Int. Ed.*, 2020, **59**, 7069–7075.
75 H. Shi, C. Imberti and P. J. Sadler, *Inorg. Chem. Front.*, 2019, **6**, 1623–1638.
76 J. Huang, W. Ding, X. Zhu, B. Li, F. Zeng, K. Wu, X. Wu and F. Wang, *Front. Chem.*, 2022, **10**, 876410.
77 E. Shaili, L. Salassa, J. A. Woods, G. Clarkson, P. J. Sadler and N. J. Farrer, *Chem. Sci.*, 2019, **10**, 8610–8617.
78 R. Czarnomysy, D. Radomska, A. Muszyńska, J. M. Hermanowicz, I. Prokop, A. Bielawska and K. Bielawski, *Molecules*, 2020, **25**, 2860.
79 R. Navarro-Peñaloza, B. Landeros-Rivera, H. López-Sandoval, R. Castro-Ramírez and N. Barba-Behrens, *Coord. Chem. Rev.*, 2023, **494**, 215360.
80 P. J. Jenks, *Infect. Dis.*, 2010, 1413–1414.
81 H. Shi, G. J. Clarkson and P. J. Sadler, *Inorg. Chem. Front.*, 2024, **11**, 7898–7909.
82 W. W.-Y. Yim and N. Mizushima, *Cell Discovery*, 2020, **6**, 6.
83 N. Mizushima, B. Levine, A. M. Cuervo and D. J. Klionsky, *Nature*, 2008, **451**, 1069–1075.
84 S. Fulda, A. M. Gorman, O. Hori and A. Samali, *Int. J. Cell Biol.*, 2010, **2010**, 214074.
85 B. Linder and D. Kögel, *Biology*, 2019, **8**, 82.
86 A. M. Cuervo, *Nat. Cell Biol.*, 2010, **12**, 735–737.
87 J. Chicote, V. J. Yuste, J. Boix and J. Ribas, *Front. Pharmacol.*, 2020, **11**, 580343.
88 T. Lamark, V. Kirkin, I. Dikic and T. Johansen, *Cell Cycle*, 2009, **8**, 1986–1990.
89 V. Kirkin and V. V. Rogov, *Mol. Cell*, 2019, **76**, 268–285.
90 Q. Chen, J. Kang and C. Fu, *Signal Transduction Targeted Ther.*, 2018, **3**, 18.
91 P. S. Felder, S. Keller and G. Gasser, *Adv. Ther.*, 2020, **3**, 1900139.
92 J. Zhu, J. Á. Rodríguez-Corrales, R. Prussin, Z. Zhao, A. Dominijanni, S. L. Hopkins, B. S. J. Winkel, J. L. Robertson and K. J. Brewer, *Chem. Commun.*, 2017, **53**, 145–148.

93 K. Sakai, H. Ozawa, H. Yamada, T. Tsubomura, M. Hara, A. Higuchi and M.-A. Haga, *Dalton Trans.*, 2006, 3300–3305.
94 A. Jain, J. Wang, E. R. Mashack, B. S. J. Winkel and K. J. Brewer, *Inorg. Chem.*, 2009, **48**, 9077–9084.
95 S. Singh, M. Varma, B. Shravage, P. Kulkarni and A. Kumbhar, *J. Chem. Sci.*, 2021, **133**, 89.
96 G. Das, B. V. Shravage and E. H. Baehrecke, *Cold Spring Harbor Perspect. Biol.*, 2012, **4**, a008813.
97 B. M. Gąsiorkiewicz, P. Koczurkiewicz-Adamczyk, K. Piska and E. Pękala, *Invest. New Drugs*, 2021, **39**, 538–563.
98 J. Šima, *Coord. Chem. Rev.*, 2006, **250**, 2325–2334.
99 A. F. Westendorf, J. A. Woods, K. Korpis, N. J. Farrer, L. Salassa, K. Robinson, V. Appleyard, K. Murray, R. Grünert, A. M. Thompson, P. J. Sadler and P. J. Bednarski, *Mol. Cancer Ther.*, 2012, **11**, 1894–1904.
100 W. Zhang, P. Gou, J.-M. Dupret, C. Chomienne and F. Rodrigues-Lima, *Transl. Oncol.*, 2021, **14**, 101169.
101 S. Jamil, I. Lam, M. Majd, S.-H. Tsai and V. Duronio, *Cancer Cell Int.*, 2015, **15**, 79.
102 S. J. Dixon, K. M. Lemberg, M. R. Lamprecht, R. Skouta, E. M. Zaitsev, C. E. Gleason, D. N. Patel, A. J. Bauer, A. M. Cantley, W. S. Yang, B. Morrison and B. R. Stockwell, *Cell*, 2012, **149**, 1060–1072.
103 Y. Mou, J. Wang, J. Wu, D. He, C. Zhang, C. Duan and B. Li, *J. Hematol. Oncol.*, 2019, **12**, 34.
104 W. S. Yang, K. J. Kim, M. M. Gaschler, M. Patel, M. S. Shchepinov and B. R. Stockwell, *Proc. Natl. Acad. Sci. U. S. A.*, 2016, **113**, E4966–E4975.
105 R. Shah, M. S. Shchepinov and D. A. Pratt, *ACS Cent. Sci.*, 2018, **4**, 387–396.
106 B. Lu, X. B. Chen, M. D. Ying, Q. J. He, J. Cao and B. Yang, *Front. Pharmacol.*, 2018, **8**, 992.
107 P. Maher, *Ageing Res. Rev.*, 2005, **4**, 288–314.
108 S. Li, H. Yuan, Y. Chen and Z. Guo, *Fundam. Res.*, 2023, **3**, 525–528.
109 Y. Qiu, Y. Cao, W. Cao, Y. Jia and N. Lu, *Pharmacol. Res.*, 2020, **159**, 104919.
110 Y. Yu, Y. Yan, F. Niu, Y. Wang, X. Chen, G. Su, Y. Liu, X. Zhao, L. Qian, P. Liu and Y. Xiong, *Cell Death Discovery*, 2021, **7**, 193.
111 S. Doll, F. P. Freitas, R. Shah, M. Aldrovandi, M. C. da Silva, I. Ingold, A. Goya Grocin, T. N. X. da Silva, E. Panzilius, C. H. Scheel, A. Mourão, K. Buday, M. Sato, J. Wanninger, T. Vignane, V. Mohana, M. Rehberg, A. Flatley, A. Schepers, A. Kurz, D. White, M. Sauer, M. Sattler, E. W. Tate, W. Schmitz, A. Schulze, V. O'Donnell, B. Proneth, G. M. Popowicz, D. A. Pratt, J. P. F. Angeli and M. Conrad, *Nature*, 2019, **575**, 693–698.
112 J. Garcia-Bermudez, L. Baudrier, E. C. Bayraktar, Y. Shen, K. La, R. Guarecuco, B. Yucel, D. Fiore, B. Tavora, E. Freinkman, S. H. Chan, C. Lewis, W. Min, G. Inghirami, D. M. Sabatini and K. Birsoy, *Nature*, 2019, **567**, 118–122.
113 K. Hadian, *Biochemistry*, 2020, **59**, 637–638.
114 Y. Lv, M. Wu, Z. Wang and J. Wang, *Cell Biol. Toxicol.*, 2023, **39**, 827–851.
115 X. Jiang, B. R. Stockwell and M. Conrad, *Nat. Rev. Mol. Cell Biol.*, 2021, **22**, 266–282.
116 Z. Xie, H. Hou, D. Luo, R. An, Y. Zhao and C. Qiu, *Inflammation*, 2021, **44**, 35–47.
117 J. Li, F. Cao, H.-L. Yin, Z.-J. Huang, Z.-T. Lin, N. Mao, B. Sun and G. Wang, *Cell Death Discovery*, 2020, **11**, 88.
118 X. Zheng, M. Liu, Y. Wu, Y. Chen, W. He and Z. Guo, *RSC Chem. Biol.*, 2024, **5**, 141–147.
119 A. Turksoy, D. Yildiz and E. U. Akkaya, *Coord. Chem. Rev.*, 2019, **379**, 47–64.
120 C. Li, J. Li, Y. Pang, L. Mei, W. Xu, Z. Zhang, C. Han and Y. Sun, *Chem. Eng. J.*, 2024, **498**, 155471.
121 D. Cui, J. Huang, X. Zhen, J. Li, Y. Jiang and K. Pu, *Angew. Chem., Int. Ed.*, 2019, **58**, 5920–5924.
122 Y. Wu, Y. Yin, S. Wang, H. Yu, Y. Ai, Y. Yuan and R. Hu, *Dyes Pigm.*, 2025, **240**, 112862.
123 M. Patra and G. Gasser, *Nat. Rev. Chem.*, 2017, **1**, 0066.
124 S. Peter and B. A. Aderibigbe, *Molecules*, 2019, **24**, 3604.
125 H. Shi, F. Ponte, J. S. Grewal, G. J. Clarkson, C. Imberti, I. Hands-Portman, R. Dallmann, E. Sicilia and P. J. Sadler, *Chem. Sci.*, 2024, **15**, 4121–4134.
126 H. Li, T. Yang, J. Zhang, K. Xue, X. Ma, B. Yu and X. Jin, *Cell Death Discovery*, 2024, **10**, 32.
127 A. Zychlinsky, M. C. Prevost and P. J. Sansonetti, *Nature*, 1992, **358**, 167–169.
128 R. Guo, H. Wang and N. Cui, *Mediators Inflammation*, 2021, **2021**, 9925059.
129 Y. Fang, S. Tian, Y. Pan, W. Li, Q. Wang, Y. Tang, T. Yu, X. Wu, Y. Shi, P. Ma and Y. Shu, *Biomed. Pharmacother.*, 2020, **121**, 109595.
130 P. Yu, X. Zhang, N. Liu, L. Tang, C. Peng and X. Chen, *Signal Transduction Targeted Ther.*, 2021, **6**, 128.
131 Y. Zheng, K. Peng, Q. Cao and Z. W. Mao, *Angew. Chem., Int. Ed.*, 2025, **64**, e202507186.
132 Q. Wang, Y. Wang, J. Ding, C. Wang, X. Zhou, W. Gao, H. Huang, F. Shao and Z. Liu, *Nature*, 2020, **579**, 421–426.
133 S. S. Wright, P. Kumari, V. Fraile-Ágreda, C. Wang, S. Shivcharan, S. Kappelhoff, E. G. Margheritis, A. Matz, S. O. Vasudevan, I. Rubio, M. Bauer, B. Zhou, S. K. Vanaja, K. Cosentino, J. Ruan and V. A. Rathinam, *Cell*, 2025, **188**, 280–291.
134 J. Liu, J. Zhou, Y. Luan, X. Li, X. Meng, W. Liao, J. Tang and Z. Wang, *Cell Commun. Signaling*, 2024, **22**, 22.
135 W. Zhang, G. Li, R. Luo, J. Lei, Y. Song, B. Wang, L. Ma, Z. Liao, W. Ke, H. Liu, W. Hua, K. Zhao, X. Feng, X. Wu, Y. Zhang, K. Wang and C. Yang, *Exp. Mol. Med.*, 2022, **54**, 129–142.
136 X. Hu, H. Zhang, Q. Zhang, X. Yao, W. Ni and K. Zhou, *J. Neuroinflammation*, 2022, **19**, 242.
137 L. Y. Liu, H. Fang, Q. Chen, M. H.-Y. Chan, M. Ng, K.-N. Wang, W. Liu, Z. Tian, J. Diao, Z. W. Mao and V. W.-W. Yam, *Angew. Chem., Int. Ed.*, 2020, **59**, 19229–19236.
138 Y. F. Zhong, H. Zhang, W. T. Liu, X. H. Zheng, Y. W. Zhou, Q. Cao, Y. Shen, Y. Zhao, P. Z. Qin, L.-N. Ji and Z. W. Mao, *Chem. – Eur. J.*, 2017, **23**, 16442–16446.
139 Y. Y. Ling, X. Y. Xia, L. Hao, W. J. Wang, H. Zhang, L. Y. Liu, W. Liu, Z. Y. Li, C. P. Tan and Z. W. Mao, *Angew. Chem., Int. Ed.*, 2022, **61**, e202210988.
140 J. J. Wilson and S. J. Lippard, *Chem. Rev.*, 2014, **114**, 4470–4495.
141 H. C. Tai, Y. Zhao, N. J. Farrer, A. E. Anastasi, G. Clarkson, P. J. Sadler and R. J. Deeth, *Chem. – Eur. J.*, 2012, **18**, 10630–10642.
142 F. Juliá, *ChemCatChem*, 2022, **14**, e202200916.
143 Q. Zhou, N.-H. Chu, J. Xu, K.-C. Law and G. Zhu, *Inorg. Chem. Front.*, 2026, DOI: 10.1039/D6QI00078A.
144 N. Casares, M. O. Pequignot, A. Tesniere, F. Ghiringhelli, S. Roux, N. Chaput, E. Schmitt, A. Hamai, S. Hervas-Stubbs, M. Obeid, F. Coutant, D. Métivier, E. Pichard, P. Aucouturier, G. Pierron, C. Garrido, L. Zitvogel and G. Kroemer, *J. Exp. Med.*, 2005, **202**, 1691–1701.
145 N. Yatim, S. Cullen and M. L. Albert, *Nat. Rev. Immunol.*, 2017, **17**, 262–275.
146 L. Galluzzi, I. Vitale, S. Warren, S. Adjemian, P. Agostinis, A. B. Martinez, T. A. Chan, G. Coukos, S. Demaria, E. Deutsch, D. Draganov, R. L. Edelson, S. C. Formenti, J. Fucikova, L. Gabriele, U. S. Gaipl, S. R. Gameiro, A. D. Garg, E. Golden, J. Han, K. J. Harrington, A. Hemminki, J. W. Hodge, D. M. S. Hossain, T. Illidge, M. Karin, H. L. Kaufman, O. Kepp, G. Kroemer, J. J. Lasarte, S. Loi, M. T. Lotze, G. Manic, T. Merghoub, A. A. Melcher, K. L. Mossman, F. Prosper, Ø. Rekdal, M. Rescigno, C. Riganti, A. Sistigu, M. J. Smyth, R. Spisek, J. Stagg, B. E. Strauss, D. Tang, K. Tatsuno, S. W. van Gool, P. Vandenabeele, T. Yamazaki, D. Zamarin, L. Zitvogel, A. Cesano and F. M. Marincola, *J. Immunother. Cancer*, 2020, **8**, e000337.
147 D. V. Krysko, A. D. Garg, A. Kaczmarek, O. Krysko, P. Agostinis and P. Vandenabeele, *Nat. Rev. Cancer*, 2012, **12**, 860–875.
148 J. X. Zou, M. R. Chang, N. A. Kuznetsov, J. X. Kee, M. V. Babak and W. H. Ang, *Chem. Sci.*, 2025, **16**, 6160–6187.
149 Y. Zhang, B.-T. Doan and G. Gasser, *Chem. Rev.*, 2023, **123**, 10135–10155.
150 I. Martins, Y. Wang, M. Michaud, Y. Ma, A. Q. Sukkurwala, S. Shen, O. Kepp, D. Métivier, L. Galluzzi, J.-L. Perfettini, L. Zitvogel and G. Kroemer, *Cell Death Differ.*, 2014, **21**, 79–91.
151 G. Kroemer, L. Galluzzi, O. Kepp and L. Zitvogel, *Annu. Rev. Immunol.*, 2013, **31**, 51–72.
152 L. Zhang, N. Montesdeoca, J. Karges and H. Xiao, *Angew. Chem., Int. Ed.*, 2023, **62**, e202300662.
153 A. Tesniere, F. Schlemmer, V. Boige, O. Kepp, I. Martins, F. Ghiringhelli, L. Aymeric, M. Michaud, L. Apetoh, L. Barault,

J. Mendiboure, J.-P. Pignon, V. Jooste, P. van Endert, M. Ducreux, L. Zitvogel, F. Piard and G. Kroemer, *Oncogene*, 2010, **29**, 482–491.
154 I. Martins, O. Kepp, F. Schlemmer, S. Adjemian, M. Tailler, S. Shen, M. Michaud, L. Menger, A. Gdoura, N. Tajeddine, A. Tesniere, L. Zitvogel and G. Kroemer, *Oncogene*, 2011, **30**, 1147–1158.
155 V. Novohradsky, J. Pracharova, J. Kasparkova, C. Imberti, H. E. Bridgewater, P. J. Sadler and V. Brabec, *Inorg. Chem. Front.*, 2020, **7**, 4150–4159.
156 Z. Deng, N. Wang, Y. Liu, Z. Xu, Z. Wang, T.-C. Lau and G. Zhu, *J. Am. Chem. Soc.*, 2020, **142**, 7803–7812.
157 D. Dersh, J. Hollý and J. W. Yewdell, *Nat. Rev. Immunol.*, 2021, **21**, 116–128.
158 X. Chen, Q. Lu, H. Zhou, J. Liu, B. Nadorp, A. Lasry, Z. Sun, B. Lai, G. Rona, J. Zhang, M. Cammer, K. Wang, W. Al-Santli, Z. Ciantra, Q. Guo, J. You, D. Sengupta, A. Boukhris, H. Zhang, C. Liu, P. Cresswell, P. L. M. Dahia, M. Pagano, I. Aifantis and J. Wang, *Cell*, 2023, **186**, 3903–3920.
159 L.-Y. Liu, J. Li, P. Sun, W. Yu, T.-Z. Ma, Y.-L. Zeng, Z. Zhao, Q. Wei, Y. Liu, J. P. Li, Z.-W. Mao and Z. Guo, *J. Med. Chem.*, 2026, **69**, 4629–4641.

